University of Crete, Department of Biology

IMBB - FORTH

A QCM-D STUDY OF THE INTERACTIONS OF INTERCALATING MOLECULES WITH DNA

GIARMATZIADIS SOFIA

Biosensors lab

Supervisor: Professor Dr. Electra Gizeli

Heraklion 2016 – 2017

CONTENTS

ABSTRACT

Small molecules that interact with DNA have been used in the form of dyes, therapeutic agents for different diseases and in diagnostic applications throughout the years. All these drugs interact with DNA either covalently or non-covalently. Intercalation, a non-covalent type of binding, generally causes stabilization, local unwinding and lengthening in the DNA, but also interrupt some other biological functions. Ethidium bromide (EtBr), a typical example of mono-intercalator, is a widely-known trypanocidal drug which has been found to inhibit nucleic acid synthesis in a variety of organisms. GelRed, in the contrary, is a bis-intercalator designed with the purpose of replacing the highly toxic ethidium bromide (EtBr) in gel electrophoresis. To find the mechanism of binding of those small molecules to nucleic acids, several experimental studies have been performed. In this study, we wanted to monitor the structural changes in DNA molecules, after the binding of both ethidium bromide and GelRed with the use of a label-free acoustic technique, the quartz crystal microbalance (QCM-D). Measurements of the acoustic ratio ΔD/ΔF of the dsDNA molecules of various lengths, in combination with the "discrete molecule binding" approach are used to confirm the elongation of the DNA in the case of ethidium bromide. A further study of the mechanism of binding of GelRed with the DNA double helix is necessary. Spectrophotometric experiments were also carried out to study the binding kinetics of the two different agents and finally atomic force microscopy (AFM) experiments have confirmed the above mentioned elongation. To conclude, our results suggest that DNA elongation can be detected with a much easier and non-invasive method and this will further help in better and more efficient drug design and in the fields of acoustic biophysics and Nano biotechnology.

INTRODUCTION

Many natural compounds interact strongly and specifically with nucleic acids, particularly with DNA. These drugs range from potential anticancer and antibiotic compounds, to agents that are used as fluorescent stains for DNA. After the discovery of the first "magic bullet" (meaning substances which could discriminate between the metabolism of the host and parasite and specifically attach the later) from the father of chemotherapy, Paul Ehrlich, which was used for the treatment of syphilis (Ehrlich, 1911), there was a massive use of dyes as therapeutic agents. However, their exact mechanism of action was remained unknown till the discovery of the structure and function of DNA, which is one of the most important discoveries of the last century (Watson and Crick, 1953). Since then, increased attention has been focused on the ways in which drugs interact with biological systems, with the goal of understanding the toxic as well as the chemotherapeutic effects of these small molecules. Consequently, there is a continuous effort in discovering new drugs that can affect DNA and follow Lipinski's "Rule of Five" at the same time (Lipinski et al, 2004). According to this rule, a compound with a good pharmacokinetic should obey at least three of the following parameters.

- Its molecular weight is less than 500
- The compound's lipophilicity, expressed as log P is less than 5
- The number of hydrogen bond donors is less than 5
- The number of hydrogen bond acceptors is less than 10

All drugs can interact with DNA in two different ways covalently and non-covalently.

1. Covalent binding in DNA is irreversible and leads to complete inhibition of DNA functions and consequently cell death. The most famous covalent binder is cisplatin, which is used as anticancer drug. When cisplatin passes the cell membrane the reduced intracellular chloride concentration allows the chloride ligands to be replaced by water molecules to form cis-$[Pt\ (H_2O)\ (NH_3)_2Cl]^{+}$ and cis-$[Pt\ (H_2O)_2\ (NH_3)_2]^{2+}$. It is generally accepted that these two cations bind covalently to the electron-rich sites on DNA such as N-donor groups. The preferred target in DNA is guanine (G) since it has the highest electron density of all four nucleobases (Johnson et al, 1989). Apart from cisplatin, other covalent binders are mitomycin C and anthramycin (Figure 1). Finally, another type of covalent binders are called alkylating agents. These agents are capable of attaching an alkyl- or methyl- group on DNA.

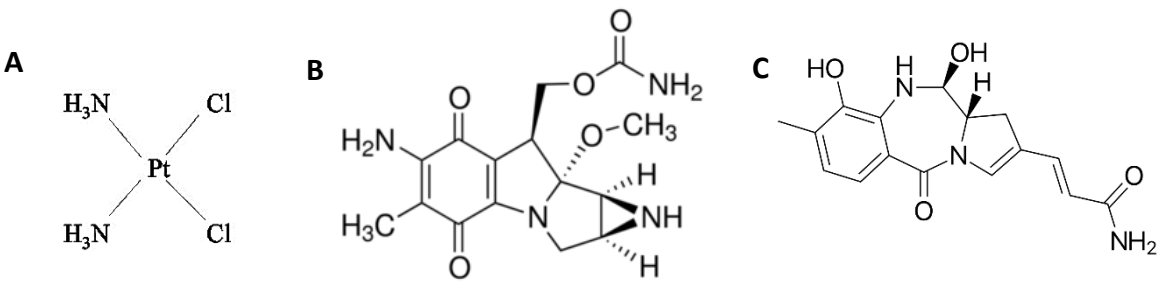

Figure 1: Chemical structure of **A)** Cisplatin, **B)** Mitomycin C and **C)** Anthramycin

2. On the other hand, **non-covalent binding** of drugs to DNA can be reversible and more desirable comparing to covalent. There are two major classes of DNA binding compounds: those that bind by intercalation and those that attach to DNA double helix externally or on one of its grooves (Figure 2).

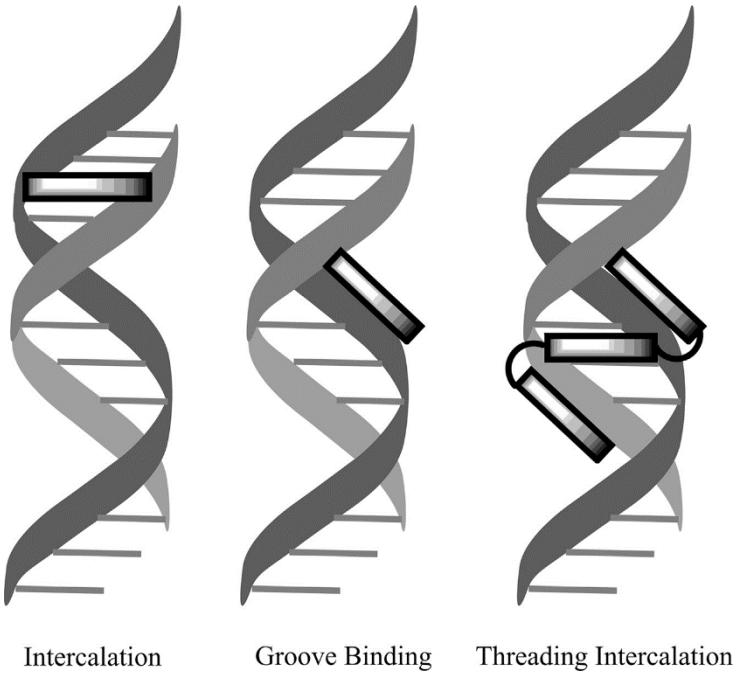

Figure 2: Schematic representation of classical intercalation, groove binding and threading intercalation mode of DNA as presented by Rescifina et al, 2014

2.1 **Major and Minor Groove binders**

Most of the DNA groove binding drugs choose minor groove as a target. They mainly have arc shape so that they can bind the curvature of the double helix, via van der Waals and electrostatic interactions (Lauria et al, 2007). Typical examples of minor groove binders are netropsin, berenil, distamycin and mithramycin (Figure 3).

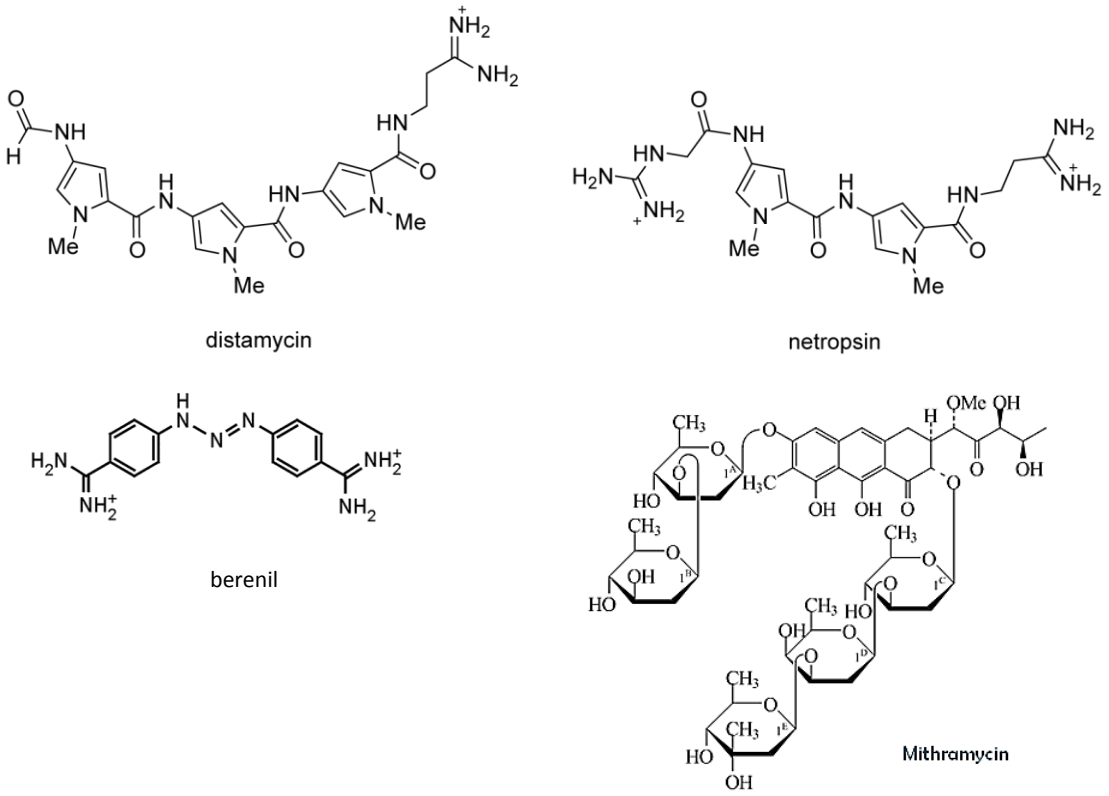

Figure 3: Chemical structure of Minor Groove Binders

Noticeably small number of substances are reported to bind major groove. The physical explanation for this phenomenon is the architecture of the double helix. Nitrogen and oxygen atoms in base pairs of the major groove are oriented in axis of the helix, which makes them accessible for specific binding interactions with proteins. In order to inhibit these protein-DNA interactions, a better understanding of the DNA- ligand interactions is necessary.

2.2 External binders

Some ligands are capable of forming non-specific, stacking interactions not with the DNA double helix or its grooves but with the DNA phosphate backbone. They can self-associate to form higher-order aggregates, which can stack on the anionic DNA backbone in order to reduce charge repulsion between ligand molecules. This way of binding was suggested for $[Ru(bpy)_3]^{2+}$ or some cations like Mg^{2+} (Kelly et al, 1985).

2.3 Intercalators

In intercalation hypothesis, a flat, usually heteoaromatic polycyclic ring is inserted between two base pairs in the double helix with a particular mode of movement (Figure 4) (Lerman et al, 1961). Stacking parallel to its neighboring base pairs, the intercalated residue lengthens the DNA double helix by approximately 1bp spacing (0.34 nm) and also produces substantial unwinding of the helix. Intercalators can be mono- or bis-intercalators, depending on the number of aromatic moieties, as well as threading intercalators.

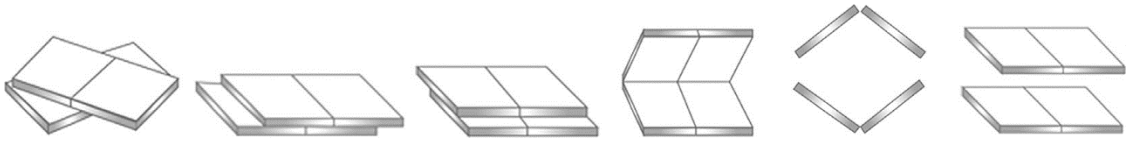

Figure 4: Movements of base pairs during intercalation; from left to right: twist, slide, shift, roll, negative cup, rise as presented by Rescifina et al, 2014.

2.3.1 Mono-intercalators

Mono-intercalators are small organic molecules with one planar moiety that intercalate between base pairs of DNA from either the major or the minor groove. There is a wide range of mono-intercalators like acridine, quinoline, phenazine, indole and penanthridine derivatives. Acridine derivatives are one of the oldest and well-studied chemotherapeutic compounds. They are widely used as antimalarial, antibacterial and antiviral agents. In general their mechanism of action is blocking DNA replication, transcription or DNA repair (Wainwright et al, 2001). Proflavine, acriflavine, euflavine, aminacrine and ethacridine provide the best examples of this group (Figure 5).

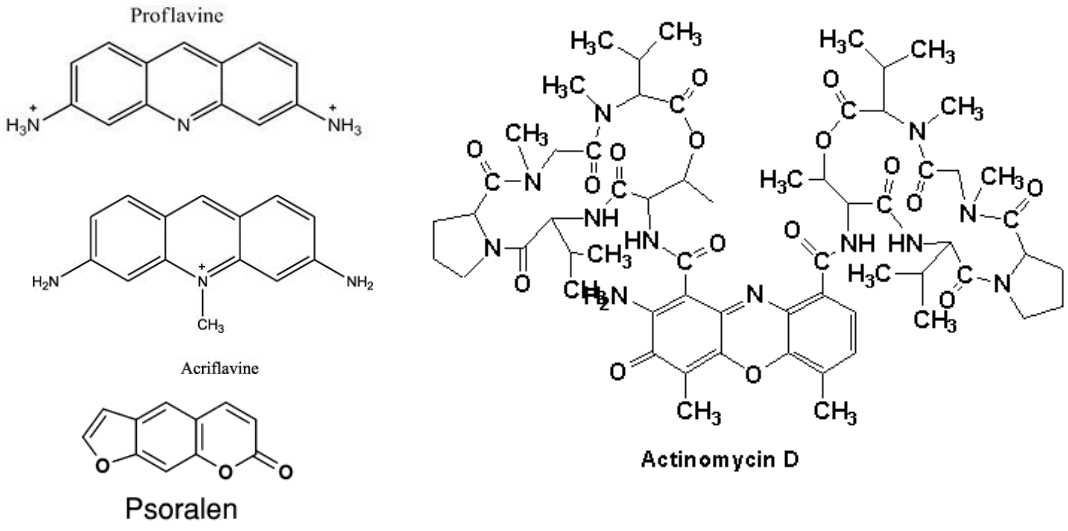

Figure 5: Selected DNA intercalating agents

- **Ethidium Bromide**

Penanthridine derivatives like ethidium bromide, quinacrine, and actinomycin are important as trypanocides. However, the biochemistry of their action seems to be very much the same as acridines (Waring et al, 1968). Ethidium bromide (EtBr) is a widely-known trypanocidal drug which has been found to inhibit nucleic acid synthesis in a variety of organisms (Figure 6) (Newton et al, 1957). It binds strongly to DNA and this binding is sensitive to increases in the salt concentration of the medium, i.e. addition of magnesium ions reduces the interaction (Waring et al, 1965).

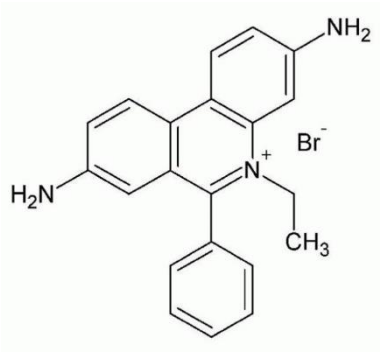

Figure 6: Chemical structure of ethidium bromide

Study of its structure is of vital importance, since it is the basis to understand the spectroscopic properties, binding specificity, hydrodynamic and dynamic characteristics. Much of our understanding of the structural details of EtBr bound to nucleic acids derived from X-ray analyses of the crystalline complexes (Jain et al, 1984). A consequence of ethidium bromide intercalation is a C2`-endo puckering of the 5`-ribosyl moiety and a C3`-endo puckering of the 3`-ribosyl moiety (Leroy et al, 1975). Such mixed sugar puckering approximately doubles the vertical separation of the bases to 6.7Å (Figure 7) (Jain et al, 1984) and leads to an unwinding of the minor groove by 26^{o} (Leroy et al, 1975). However, these conformational changes are not permanent since the complex formation with ethidium bromide does not lead to irreversible distortion of the DNA structure (Waring et al, 1965).

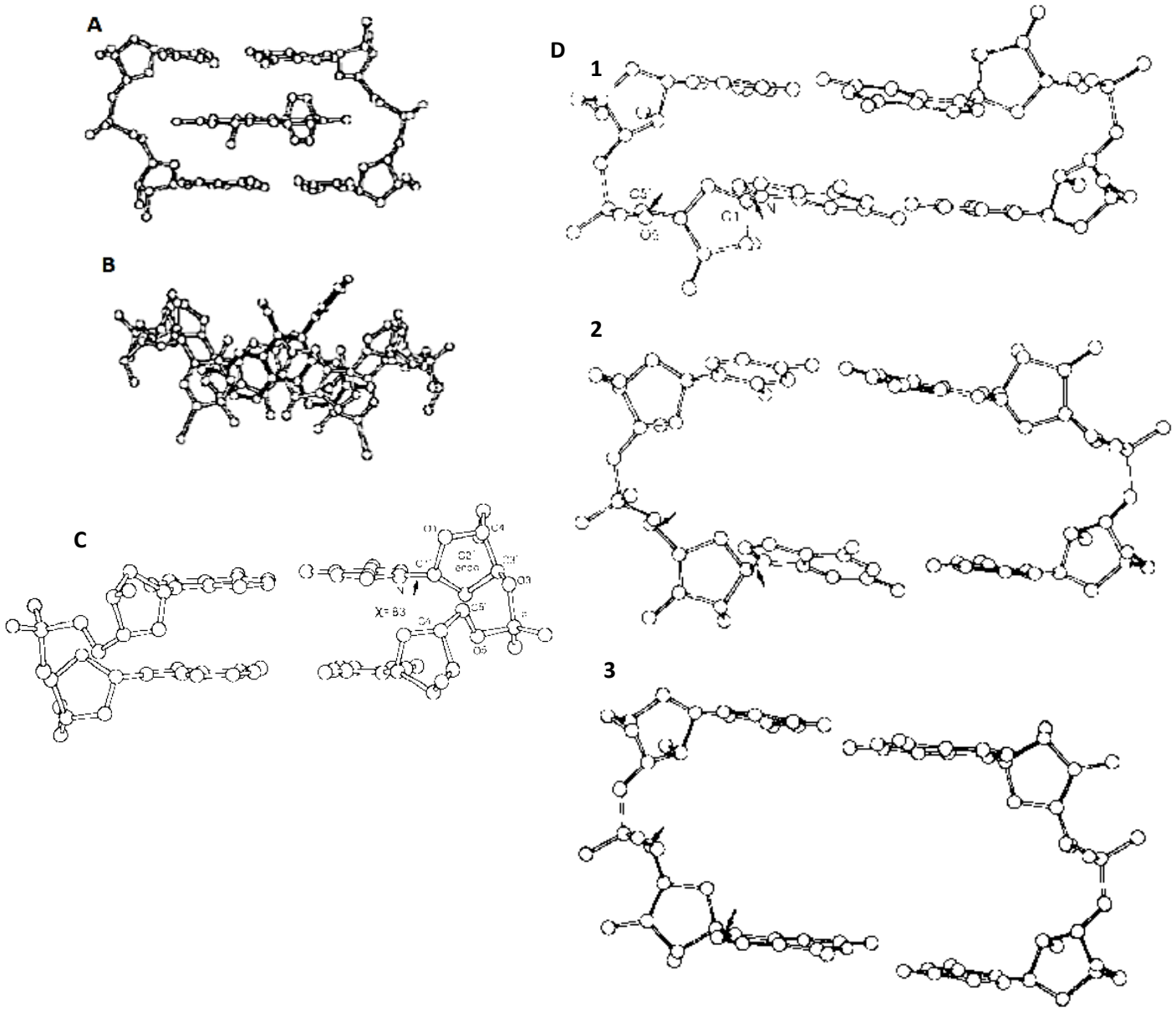

Figure 7: An i5CpG phosphate complex with ethidium bromide viewed from side **(A)** and from upper part **(B)**, compared to the structure of the B form of DNA **(C)**. The transition from an A conformation to the intercalated geometry **(D 1→3)**

2.3.2 Bis-intercalators

Bifunctional intercalators are formed from two mono-intercalators joined together through a covalent linkage. The linkage between the two mono-intercalators should be optimal in length to allow the two mono-intercalators to insert and form stacking interactions with the base pairs. Bis-daunomycin, Triostin A, YOYO, TOTO, Ethidium homodimer (EthD), GelRed and Echinomycin are examples of this class (Figure 8). Bifunctional intercalators are able to insert to DNA molecule in two different ways: through intramolecular and intremolecular cross linking depending on the number of DNA molecules that interact with the bifunctional intercalator (Figure 9) (Aleksic et al, 2014).

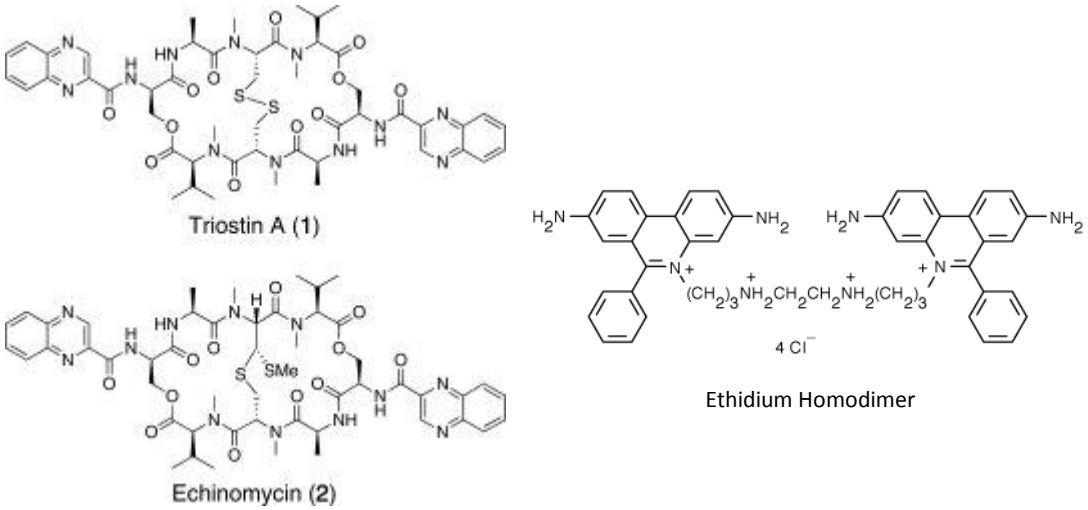

Figure 8: Selected Bis-intercalators

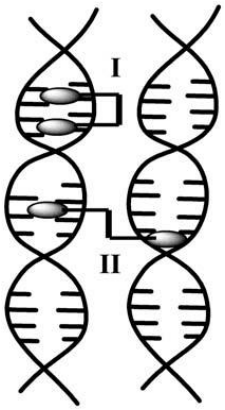

Figure 9: Types of intercalation of bifunctional intercalators in DNA molecule: I - intramolecular cross-link and II – intermolecular cross-link, as presented by Aleksic et al, 2014.

- **GelRed**

GelRed is a fluorescent nucleic acid stain designed with the purpose of replacing highly toxic ethidium bromide (EtBr) in gel electrophoresis and other experimental techniques which depend on the fluorescence of stained DNA. GelRed has the same absorption and emission spectra as EtBr and the compound can be used in electrophoresis with greater sensitivity than EtBr, plus with the advantage of being much less toxic and mutagenic (Fei et al, 2006). This last property is because the chemical structure of the dye was designed such that the dye is incapable of crossing cell membranes. The chemical structure of GelRed is synthesized by linking two EtBr molecules with a linear spacer as shown in figure 10.

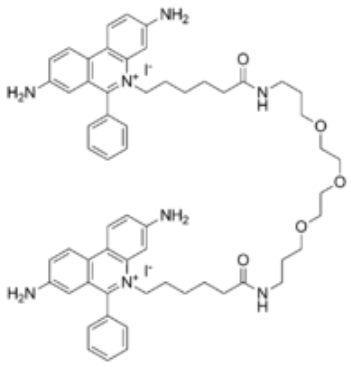

Figure 10: Structure of GelRed as presented by Fei et al, 2006

2.3.3 Threading intercalators

Apart from mono- and bis- intercalators there are some more complex agents like daunomycin and adriamycin. These intercalators are called threading intercalators since they carry bulky groups next to the intercalating moiety which interact strongly with both the minor and major grooves of DNA simultaneously (Tanious et al, 1991) (Figure 2 and 11).

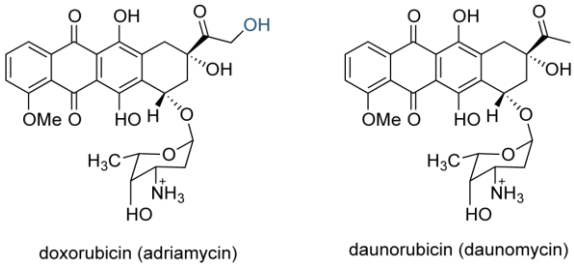

Figure 11: Chemical structure of some threading intercalators

Techniques for Detection DNA–drug Interaction

Monitoring how the binding of small molecules affects DNA conformation and viscoelastic properties is a hot field of research. Huge number of techniques are used to investigate these interactions starting from classic UV-VIS spectroscopy (Liu et al, 1996), X-ray crystallography (Egli et al, 1991), viscosity experiments (Lerman et al, 1961), dynamic light scattering (Nordmeier et al, 1992), changes in melting temperature (Xiao et al, 1994), all the way to most recent optical, electrochemical and acoustic biosensors (Sassolas et al, 2008).

- **UV-Vis spectroscopy**

UV-Vis absorption spectroscopy can detect the DNA–drug interaction by measuring the changes in the absorption properties of the drug or the DNA molecules. The UV–Vis absorption spectrum of DNA exhibits a broad band (200–350 nm) in the UV region with a maximum at 260 nm. This is the wavelength that nanodrop uses to calculate the DNA concentration. DNA–drug interactions can be studied by comparison of UV–Vis absorption spectra of the free drug and DNA–drug complexes, which are usually different (Figure 12).

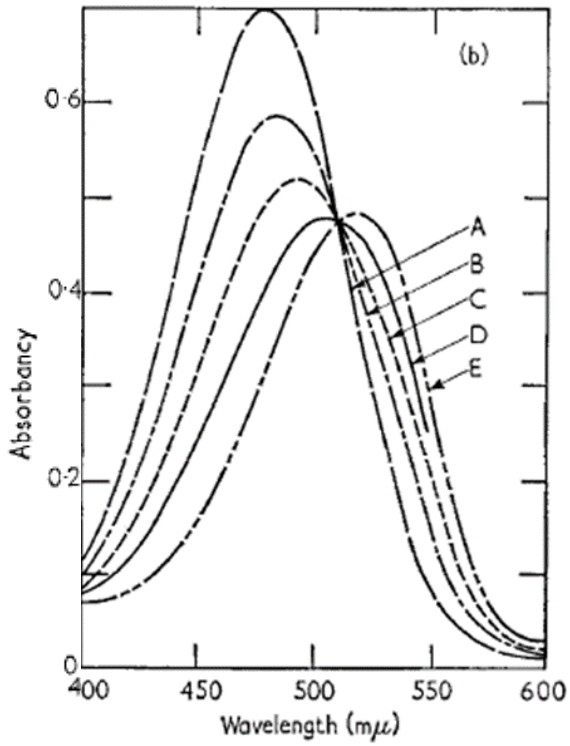

Figure 12: Schematic representation of a mixture spectrum from Waring et al, 1965 where A is the spectrum of the total free drug (in this case ethidium bromide), E is the spectrum of the total bound drug to DNA and B-D are the intermediate states

The binding process is also associated with some structural deformation and adaptation of the DNA as well as the drug molecule, in order to accommodate each other. All these processes are associated with some enthalpy and entropy changes (Breslauer et al, 1987). Since no covalent bond formation is involved, the binding can be considered as an equilibrium process, and the corresponding equilibrium constants can be determined by measuring the free and bound fraction of drug. In many cases, all the spectra in a series pass through a common point called an isosbestic point. The most common circumstance under which this obtains is when there are only two forms of the drug, in this case “free” and “bound” components.

If this happens, the reaction may be described by the following equation:

$$\text{DNA}_{\text{(free sites)}} + \text{DRUG}_{\text{(free drug)}} \leftrightarrow \text{COMPLEX}_{\text{(bound drug)}}$$

Assuming that the binding sites are independent, the association constant will be equal to:

$$K_a = \frac{[\text{bound drug}]}{[\text{free sites }][\text{free drug}]}$$

Defining the following quantities, C_1 = free drug concentration; C_2 = bound drug concentration; $C = C_1 + C_2$ = total drug concentration; (bp) = total concentration of DNA base pairs and n = number of binding sites per base pair, then:

$$K_a = \frac{C_2}{[n(bp) - C_2]C_1}$$

The bound drug concentration, C_2, can be replaced by r(bp), where r is the binding ratio, giving:

$$K_a = \frac{r}{(n-r)C_1}$$

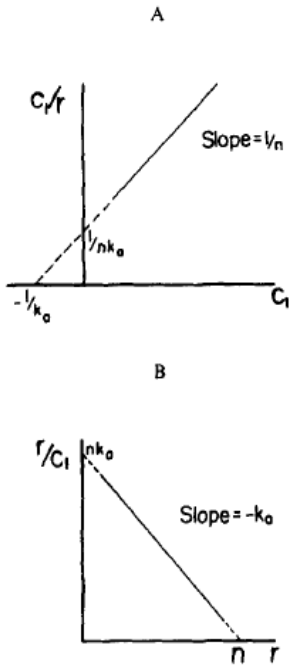

$$\frac{C}{r} = \frac{C}{n} + \frac{1}{K_a n}$$

$$\frac{r}{C_1} = K_a(n - r)$$

Figure 13: Graphical representation of two possible linear transformations of the binding equation for a single binding species

For the evaluation of the parameters n and K_a, several linear transformations of this equation have been used (Dougherty et al, 1982). Graphic representation of C_1 / r vs. C_1 or r/C_1 vs. r, leads to the so-called Scatchard plot, which is widely used (Figure 13).

However, it is possible for a bound drug to occupy more than one binding sites, due to the fact that binding at a particular site precludes binding at neighboring sites. This is called the neighbor exclusion model (Figure 14). For example, the phenyl substituent on ethidium bromide could prevent the approach, within a certain distance, of another potential binding drug.

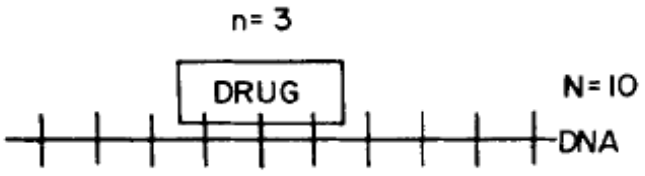

Figure 14: An example to illustrate the neighbor exclusion model as represented by Dougherty et al, 1982

Using this technique and the same way of analysis, the following table summarizes the experimental conditions - concentrations and the binding parameters between ethidium bromide and nucleic acids derived from various laboratory groups (Table 1).

PUBLICATION	IONIC STRENGTH	[EtBr] (μM)	K_a 10^6 (M^{-1})	K_d 10^{-6} (M)	n (bp)
Waring et al, 1965	40mM Tris-HCL (pH: 7.9)	125	1.4	0.7	2.27
Wu et al, 2008	50mM Tris 20mM NaCl (pH: 7.4)	2	-	-	2
Chib et al, 2014	150mM PBS	36.9	-	-	2.5
Vardevanyan et al, 2003	20mM [Na^+]	57	1.3	0.77	2.5
Nordmeier et al, 1992	10mM Tris-HCl (pH = 7.2)	460	0.18	5.55	2-2.5
Muller et al, 1975	PBS containing 7mM Na_2HPO, 2mM NaH_2P0, 180mM NaCl, 1mM EDTA (pH 7.0-7.1)	-	0.05	20	2.76
Dougherty et al, 1982	-	-	0.018	55.5	2.92
Rocha et al, 2007	140mM $NaCl_2$	20	0.15	6.66	2.5
Gaugain 1978	0.2M Na^+, 0.2M sodium acetate (pH=5)	10	0.15	6.66	2
LePecq et al, 1967	25mM Tris-HCl 0.1M NaCl pH=7.5	10^4	0.66	1.5	2.5
Macgregor et al, 1986	20mM Tris-HCl, 100mM NaCl, 1mM EDTA, pH 7.2	4	2.9	0.35	2.5
Douthart et al, 1973	50mM NaCl- 1mM Tris-1mM EDTA (pH 7)	25	4.7	0.2	2.6

Table 1: Binding parameters of EtBr to dsDNA

On the other hand, the binding of bis-intercalators with DNA is slightly different than that of mono-intecalators. Although the manufacturer states that GelRed binds to DNA by a combination of intercalation and electrostatic binding (Biotium 2013), most details of the interaction have not yet been reported in the literature. Crisafuli and his colleagues have performed two different types of experiments, single-molecule stretching and dynamic light scattering experiments to gain insight into this interaction. They found that each bound GelRed molecule effectively occupies 3.7 DNA base-pairs and increases the contour length by 0.65 nm (Crisafuli et al, 2015). These values are compatible with results expected for bis-intercalating molecules. For example, studies with Ethidium Homodimer (EthD) in solution concluded that EthD binding with dsDNA is strong with an affinity constant of 2 x 10^8 M^{-1} and that the bound dye covers 4bp (Gaugain et al, 1978).

- **Quartz Crystal Microbalance with Dissipation (QCM-D)**

The quartz crystal microbalance with dissipation monitoring (QCM-D) is a powerful tool for real-time detection of biomolecule adsorption to solid/liquid interfaces (Höök et al, 1999; Dixon, 2008). QCM-D measures the changes in the resonance frequency (ΔF) and energy dissipation (ΔD) of a sensitive quartz crystal when molecules in solution are adsorbed to its surface. The mass of the absorbed molecules can be calculated from the frequency shifts (ΔF) by utilizing the Sauerbrey equation, $\Delta m = \frac{C}{n} \Delta F$, where Δm is the mass absorbed, n is the harmonic number and C is equal to $C = \frac{t_p \rho_q}{f_0}$, where t_q being the thickness of quartz, ρ_q being the density of quartz and f_o being the resonant frequency and equals to ~ -17.7 Hz ng/cm^2 for a typical 5 MHz crystal (Sauerbrey et al, 1959; Zhang et al, 1997). The linearity of the Sauerbrey equation is valid when:

1. the added mass makes a homogenous and thin layer, which depends on the penetration constant δ (depth)
2. the added mass is rigid (D=0)
3. and no-slip conditions takes place during the quartz crystal vibrations

The viscoelastic properties of the absorbed mass can be calculated by applying the Voigt model to the frequency and dissipation data. (Voinova et al, 1999; Höök et al, 2001) The dissipation parameter is dimensionless, defined as $D = \frac{E_{Dissipated}}{2\pi E_{stored}}$, with $E_{Dissipated}$ being the energy dissipated during one oscillatory cycle and E_{stored} being the energy stored in the oscillating system. The equations of the Voigt model combine the multiple harmonic data obtained and can derive information about the constants d_f (film thickness), η_f (shear viscosity), μ_f (elastic modulus) and ρ_f (effective density) of the adlayer.

Since QCM-D measurements are non-invasive, have nanogram sensitivity and allow calculations of the viscoelastic properties of films, it has been found to be an excellent method for the analysis of DNA films (Su et al, 2005). Pope and her colleagues have exploited the fact that on the basis of the work of Sauerbrey, at 25 MHz each shift of 1 Hz in the resonant frequency of the crystal corresponds to a mass change of 3.5ngcm^{-2} and used QCM-D to show that two organic drugs, berenil and nogalamycin, have different binding properties on DNA films (Pope et al, 2001). Johal and his group, on the other hand, have reported in situ hybridization between ssDNA and its complementary strand in solution and confirmed this dsDNA formation with the help of ethidium bromide since it has higher affinity to dsDNA than ssDNA (Rawle et al, 2007; Yang et al, 2008). Okahata and his colleagues have developed a lipid- coated quartz-crystal microbalance (QCM) system, in which the adsorption behaviors of various bioactive compounds can be quantitatively detected from frequency changes in an aqueous solution (Okahata et al, 1993). They have shown that one molecule of ethidium bromide bind per 3.3 base-pairs in the DNA film and that it has an apparent

binding constant of 1.2 10^5 M^{-1}. After more than a decade the same group have examined a variety of intercalative molecules and shown that apart from the other molecules ethidium binds one per 1.6 molecules of DNA and that it occupies approximately two base pairs when it intercalates into the double helix with the maximum binding amount (Okahata et al, 2016). They have also claimed that the binding constant is around 41 10^3 M^{-1}, so ethidium can be easily removed from its complexed form. This phenomenon is in agreement with the observation of Waring that EtBr is released from its complexed form with nucleic acid after the addition of salts to the solution (Waring et al, 1965), but in contrast to Rawle, who shows that there is some irreversibility to this binding (Figure 15) (Rawle et al, 2007).

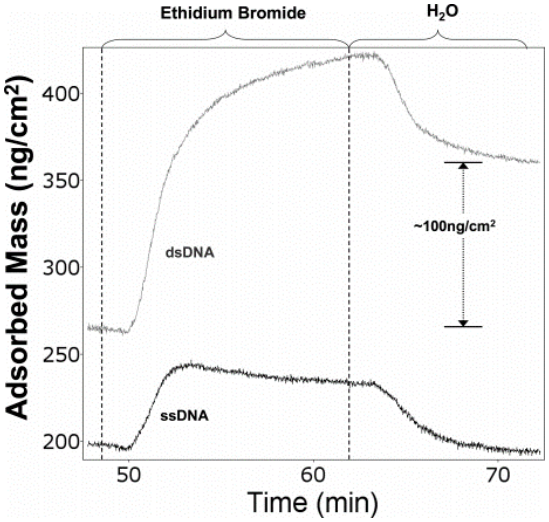

Figure 15: Calculated adsorbed mass per unit area during the exposure of ssDNA (black) or dsDNA (gray) surfaces to ethidium bromide from Rawle et al, 2007

Previous work from our lab have proposed a new mathematical treatment of the data obtained from QCM-D, which, in contrast to the Voigt model, is based on the fact that biomolecules anchored, by a single point to the surface, behave as discrete molecules and the acoustic ratio ΔD/ΔF is directly related to the intrinsic viscosity [η] of the surface-bound molecule. To explain, solution viscosity is well known to be related to the solvent viscosity (η), the concentration (C) and the intrinsic viscosity of the particular solute [η] and the Huggins constant (K_H) (Eq.1 in Figure 16). Intrinsic viscosity is related to the specific geometrical features of the molecule (i.e. length, shape). For non-interacting molecules K_H is zero so acoustic measurements can be directly related to the dissolved particle's intrinsic viscosity, as indicated by Eq. (3) in Figure 16. Consequently each molecule has its own and characteristic acoustic ratio ΔD/ΔF (Figure 16) (Tsortos et al, 2008).

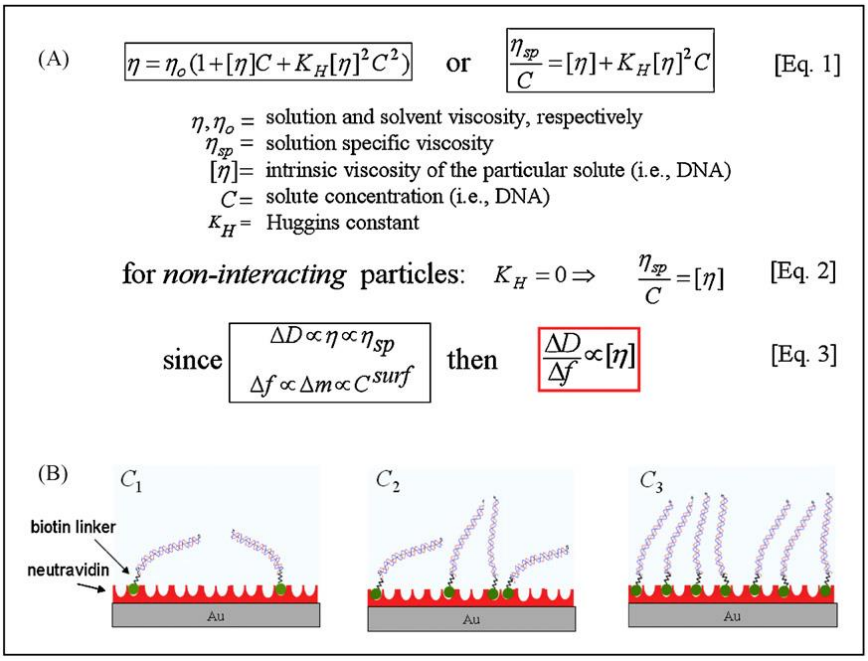

Figure 16: Correlation of classical macromolecule solution viscosity theory to acoustic measurements. Tsortos et al, 2008

Based on this theory, we exploit the capability to follow structural changes in DNA hybridization in situ and distinguish between two hybridized DNA molecules of same mass, but different shape (Papadakis et al, 2012). We have also applied this model on a wide range of DNAs of various sizes and find the relationship between acoustic ratio ΔD/ΔF (10^{-6}/Hz) and not only the intrinsic viscosity but also the length of the DNA. (Figure 17) (Tsortos et al, 2016).

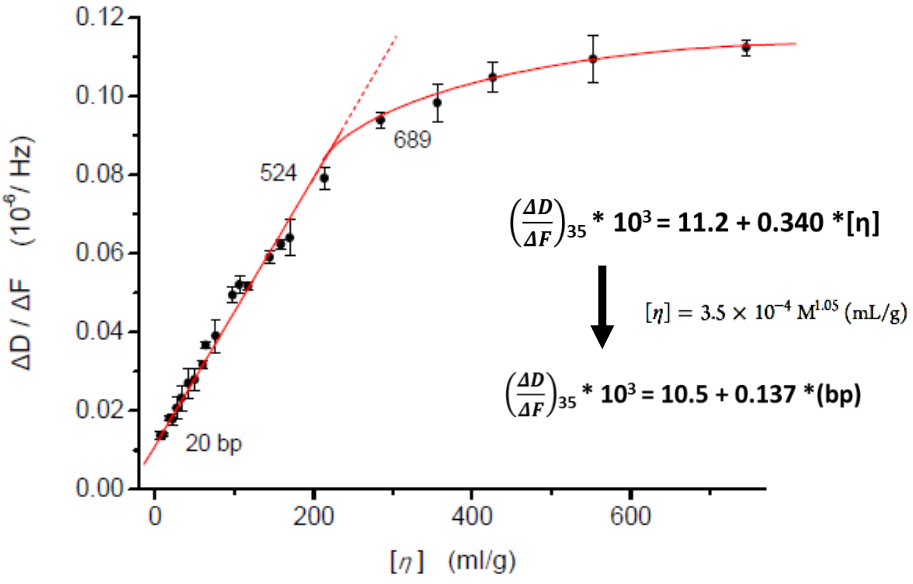

$\left(\frac{\Delta D}{\Delta F}\right)_{35} * 10^3 = 10.5 + 0.137 *(bp)$ **(Equation 1)**

Figure 17: The acoustic ratio/intrinsic viscosity relationship for linear dsDNA for the 35 MHz frequency of the QCM device and the equation derived (1). Tsortos et al, 2016

The above equation gives the ability to predict the acoustic ratio ΔD/ΔF of any length of DNA just by knowing the number of its base pairs and vice versa. This capability will be used in this study as a tool to calculate the elongation of a specific DNA molecule. Recently, we successfully checked whether this mathematical treatment of the data obtained from QCM-D can also be applied to proteins and we studied the expansion and collapse of an intrinsically disordered protein ZipA (Mateos-Gil et al, 2016).

- **Acoustic Device**

The work described here was carried out with a QCM-D acoustic device (Biolin Scientific, Stockholm, Sweden).

Figure 18: The QCM-D acoustic devise as shown in the left part of the figure and one of its chamber in the right part of the figure in which a gold quartz crystal is already placed with the electrode on the upper part

The operating frequency for the results reported is the 35 MHz overtone. To ensure a clean surface, at the beginning of each experiment, all the sensor chips, which are gold coated (Biolin Scientific, QSX301 gold, 100nm thickness), were subjected to piranha cleaning, for approximately 10 min, or plasma etching in a Harrick Plasma Flo device. Piranha is a mixture of sulfuric acid (H_2SO_4) and hydrogen peroxide (H_2O_2) [1:2], used to clean organic residues off and add -OH groups to the surfaces, making them highly hydrophilic. We have concluded that there was no difference between the two cleaning methods in the signal obtained (data not shown). After washing away any absorbed samples by the end of each experiment, using Hellmanex 2%, the surfaces were reused.

- **Design and Synthesis of dsDNA Molecules**

For the experiments analyzed above, 16 different lengths of dsDNA molecules were produced (21, 50, 88, 114, 157, 195, 250, 327, 395, 446, 635, 666, 852, 1011, 1294 and 1724 bp). DNA molecules 21 and 50 bp long were generated by hybridization of two complementary strands in PBS buffer, pH 7.4. The mixtures were heated at 95^{o}C for 5 min and cooled down at room temperature for approximately 1 hour. The sequences of these two DNA molecules are shown below:

✓ **21 bp:**
1st strand: 5`-biotin-TAGAGCTCCCTTCAATCCAAA -3`
2nd strand: 5`-TTTGGATTGAAGGGAGCTCTA -3`

✓ **50 bp:**
1st strand: 5`-biotin- AATTCAGAGAGGAGGAGAGAGCGGTGCGGTAGGAGAGAGAGAGGAGGATC-3`
2nd strand: 5`- GATCCTCCT CTCTCTCTC CTACCGCAC CGCTCTCTC CTCCTCTCT GAATT-3`

All the other DNA molecules were produced at controlled lengths by a standard Polymerase Chain Reaction using different DNA template each time and primers (biotinylated forward and reverse) purchased from Metabion (Germany), IDT (USA), Microchemistry (Heraklion) and FRIZ Biochem (Germany). For the PCR a ReadyMix PCR Kit was utilised [KAPA2G Fast HotStart, KAPAbiosystems KR0376]. The conditions for each reaction were standard, with a slight difference in the annealing temperature, ranging from 55^{o}C -62.5^{o}C and the number of cycles (35 - 40). For DNA molecules above one hundred base pairs (1011bp, 1294bp, 1724bp) a different protocol was used.

- Denaturation: 15 sec, 95^{o}C,
- Annealing: 15 sec, 60^{o}C and
- Extension: 30 sec, 72^{o}C for 30 cycles.

The corresponding molecular weights and the DNA templates employed for each DNA molecule, are given in the following table (Table 2). The PCR products were purified using nucleospin kit (Macherey-Nagel, Germany) and run through an agarose gel 2% to confirm the generation of the correct specific product. The exact concentration of each product was measured in a Nanodrop Spectrophotometer ND-1000. Molecular Weight of biotin is 244.31 gr/mol.

BASE PAIRS	M (g/mol)	Template DNA
21	12850.5	-
50	30774.1	-
88	54246.4	Salmonella Enterica DNA (1.4 ng/μL)
114	70308.8	Human DNA (BRCA1 gene/exon 20) (10ng/μL)
157	97499.4	Human DNA (BRCA1 gene/exon 20) (10ng/μL)
195	120341.6	Salmonella Enterica DNA (1.4 ng/μL)
250	154339.4	Human DNA (BRCA1 gene/exon 20) (10ng/μL)
327	202522.8	Human DNA (BRCA1 gene/exon 20) (10ng/μL)
395	243377.6	Plasmid DNA pBR322 (Minotech, Greece) (0.5ng/μL)
446	275427.2	Human DNA (BRCA1 gene/exon 20) (10ng/μL)
635	392305.8	Salmonella Enterica DNA (1.4 ng/μL)
666	411448.4	Salmonella Enterica DNA (1.4 ng/μL)
852	526396.5	Salmonella Enterica DNA (1.4 ng/μL)
1011	624641.1	Plasmid DNA pBR322 (Minotech, Greece) (0.5ng/μL)
1294	799532.8	Plasmid DNA pBR322 (Minotech, Greece) (0.5ng/μL)
1724	1065252.3	Plasmid DNA pBR322 (Minotech, Greece) (0.5ng/μL)

Table 2: The template used for the production of each dsDNA molecule and the corresponding molecular weight

PRIMERS:

- ✓ **88 bp:**

Forward: 5`- biotin - TCCTTTTCCAGATTACGCAACAGATACT-3`

Reverse: 5`- TTGGGTTCTGGATTTTTGATTATCCTGC -3`

- ✓ **114 bp:**

Forward: 5'- biotin - GCTCCACTTCCATTGAAGGAAGC - 3'

Reverse: 5'-TGGTGGTTTCTTCCATTGAC-3'

- ✓ **157 bp:**

Forward: 5`- biotin- TCCTGATGGGTTGTGTTTGG-3`

Reverse: 5`-GACAAAAATCTCACCCCACCA-3`

- ✓ **195 bp:**

Forward: 5`-biotin- GGATCACTAAGCTGTGGATTACCTATTATC-3`

Reverse: 5`-CTGTTATTTCCTGCGTGGATATTTCTTTAG-3`

- ✓ **250 bp:**

Forward: 5`- biotin - GACAAAAATCTCACCCCACCA-3`

Reverse: 5’- ACCTGTGTGAAAGTATCTAGCACTG-3’

- ✓ **327 bp:**

Forward: 5`- biotin - CCAAAGCGAGCAAGAGGATCTC -3`

Reverse: 5’- CTCATCTGCTTAAAGTCCCAGCTC -3’

- ✓ **395 bp:**

Forward: 5`- biotin - CCACCAAACGTTTCGGCGAG -3`

Reverse: 5’- GCCGGCTTCCATTCAGGTCG -3’

- ✓ **446 bp:**

Forward: 5’- biotin - GCTCCACTTCCATTGAAGGAAGC - 3’

Reverse: 5’- CTCATCTGCTTAAAGTCCCAGCTC -3’

- ✓ **635 bp:**

Forward: 5' – biotin – GACACCTCAAAAGCAGCGT - 3'

Reverse: 5'- AGACGGCGATACCCAGCGG - 3'

- ✓ **666 bp:**

Forward: 5'- biotin – GAAGCGTTAGTGAGCCGTCTGCG - 3'

Reverse: 5'- ATCAGCGACCTTAATATCTTGCCA - 3'

- ✓ **852 bp:**

Forward: 5'- biotin – GTCACGGTGATCGATCCGGT - 3'

Reverse: 5'- CACGATATTGATATTAGCCCG - 3'

- ✓ **1011 bp:**

Forward: 5`- biotin- TCTTGCTGGCGTTCGCGACG-3`

Reverse: 5’-GTCTGGCTTCTGATAAAGCGGGCC-3’

✓ **1294 bp:**

Forward: 5`- biotin- TCTTGCTGGCGTTCGCGACG-3`

Reverse: 5'- GCCAGTATACACTCCGCTATCGCTACG-3'

✓ **1724 bp:**

Forward: 5`- biotin- TCTTGCTGGCGTTCGCGACG-3`

Reverse: 5`- CCGGTAAGCGGCAGGGTCGG-3`

- **Real-Time Acoustic Detection of Neutravidin and DNA Binding**

A continuous flow of the corresponding buffer (PBS 150 mM pH 7.4 and PBS 150 mM pH 7.4 plus $MgCl_2$ 10 mM) was pumped over the gold-coated surface at a flow rate of 50 µL/min. The buffers were filtered with a PVDF (polyvinylidene Fluoride) membrane filter 0.22 µm (Millex). The signal was allowed to stabilize before and in between of every addition of samples and all the samples were added in the same buffer. At the beginning of every experiment neutravidin was added at a concentration of 200 µg/mL for 4 min, long enough to saturate the surface with a large excess of protein. Neutravidin was bought from Thermo Fisher, Invitrogen (A2667), at a concentration of 5 mg/mL. DNA biotinylated samples were added at a range of concentrations varying from 1-14 µg in final volume of 200µL depending on their length. After a buffer rinse, DNA molecules were attached to the surface through biotin-neutravidin interaction (Figure 19). Ethidium Bromide (Merck, Mr: 394.32 g/mol) was added at concentrations ranging from 0 to 200 µM in the same buffer and GelRed (Biotium), was added at the same concentrations.

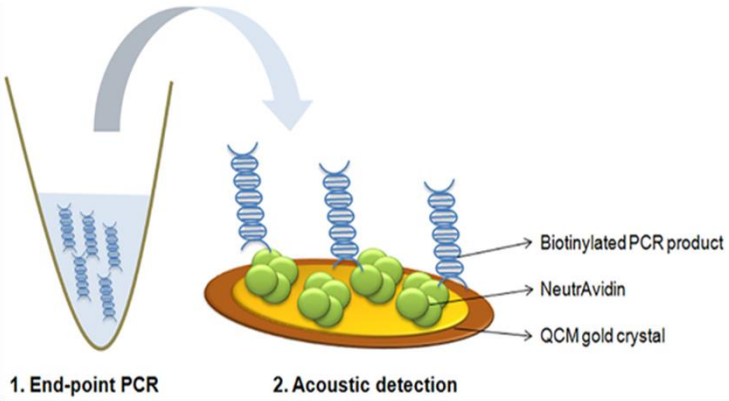

Figure 19: Experimental procedure for acoustic measurements as shown in Papadakis et al, 2015

- **Spectrophotometric Measurements**

Measurements were made in a SpectraMax M2 spectrophotometer with the use of a Hellma Suprasil-Quartz cuvette, 1cm light path (type: 105.250-QS). The technique used in these binding studies was that of Peacocke & Skerrett (Peacocke et al, 1956) for the interaction of proflavine with nucleic acids. A solution of a specific concentration of the drug containing a high concentration of nucleic acid was prepared and diluted with a solution of the drug alone at the same concentration as in the mixture. In this way measurements were made on solutions containing a fixed concentration of the drug and decreasing concentrations of nucleic acid. Before each experiment the cuvette was cleaned multiple times with ethanol 70% and distilled water from Barnstead NANOpure II filters. All readings were obtained a few minutes after mixing solutions of the drug with nucleic acid and with reference to a blank containing the buffer alone. The spectra obtained were at wavelengths in the range of 350 to 600nm and at 25^{o}C experimental temperature. Measurements were found to follow Beer`s law A=C*ε*l (A=Absorbance, C=Concentration, ε=extinction coefficient and l=light path) for all the drug concentrations used and for each ε of the drug according to its state. Ethidium bromide at 480nm has an extinction coefficient around 5700 when it is free, but 2950 when it is bound to nucleic acids (Douthart et al, 1973) (see table 2). Concentrations of the solutions were confirmed also in NanoDrop Spectrophotometer ND-1000. For this study lambda DNA was used (Minotech, 0.5mg/mL, 31.5 Mda, 48502bp) as a "model" molecule to set our experiments since it is commercially available and could give higher base pair concentrations than any PCR-produced molecule. The concentration used for each experiment was 700μM calculated in base pairs, whereas ethidium bromide was kept at 100μM and GelRed at 50μM. The treatment of the results was made in accordance to Peacocke & Skerrett analysis (Peacocke et al, 1956) and Scatchard (Scatchard, 1949) as described in the Introduction.

PUBLICATION	$\varepsilon_{ethidium}$ @480nm free (M^{-1} cm^{-1})	$\varepsilon_{ethidium}$ @480nm bound (M^{-1} cm^{-1})	$\varepsilon_{ethidium}$ @510nm (M^{-1} cm^{-1})	ε_{DNA} @260nm (M^{-1} cm^{-1})	ISOSBESTIC POINT (nm)
Wu 2008				6600	
Vardevanyan 2003	5600			6400	512
Nordmeier 1992	5600		4110	6600	510
Muller 1975				6412	
MacGregor 1986	5850				
Douthart 1973	5700	2950			510
Benevides 2005	5860			6600	
Porschke 1993	5700				

Table 3: Some of the extinction coefficient numbers found in literature

- **Atomic Force Microscopy (AFM) measurements**

High resolution atomic force microscopy (AFM) was used to visualize DNA molecules and their elongation after the treatment with the intercalators. Images were acquired in air with a NanoScopeIIIa (Digital Instruments) microscope and typical image sizes were between 1 to 3μm and 256-512 pixels. Tapping mode images were acquired using Veeco tips (RTESP-300) from Bruker with a scan rate of 1-2 Hz (nominal resonant frequency 300 KHz and nominal spring constant 40 N/m). Images were processed using "WsXM" software, freely available on internet and analyzed using "Image J" software.

An aliquot of 5μL dsDNA molecules 0.5ng/μL diluted in Tris 10mM buffer plus 9mM $MgCl_2$ was incubated onto a freshly cleaved Mica surface for 1 minute. Tris buffer was used to ensure the low salt content of the surface and $MgCl_2$ to ensure the binding of the negatively charged DNAs on the Mica. After the incubation an extensively rinsing with distilled water was followed, the excess of the liquid was blotted away with filter paper and finally the surfaces were dried gently with nitrogen. The same DNA molecules were also pre-incubated with 100μM EtBr diluted in Tris 10mM for 1 hour. 9mM $MgCl_2$ was added to these samples and the same procedure was performed for the incubation on the surfaces.

For the analysis of the images on "Image J", the scale of the images was first set to their correct dimensions, then with the use of the segmented line we drew above the DNA molecules and afterwards we fit spline. With this method we could take specific measurements of the contour length of the DNA molecules.

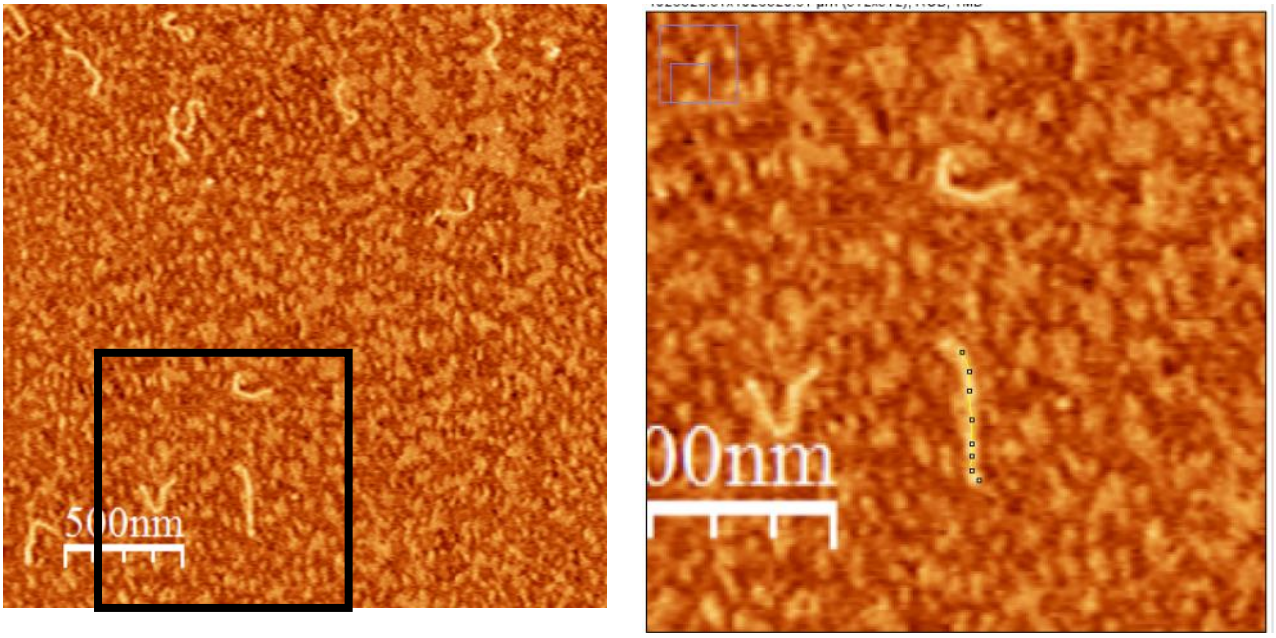

Figure 20: AFM image before (left) and after (right) the setting of the segmented line (black points on the right zoomed image)

At the beginning of this study, we wanted to make sure that the mathematical model proposed from our lab could be used also at 37°C which is biologically relevant (in contrast to 25°C from Tsortos et al, 2016 publication). We performed a series of experiments on three different lengths of linear dsDNA (114bp, 635bp, 1011bp) changing the temperature from 25°C to 37°C and backwards. As figure 21 indicates, we observed that the temperature does not affect the values of the acoustic ratios (Figure 21).

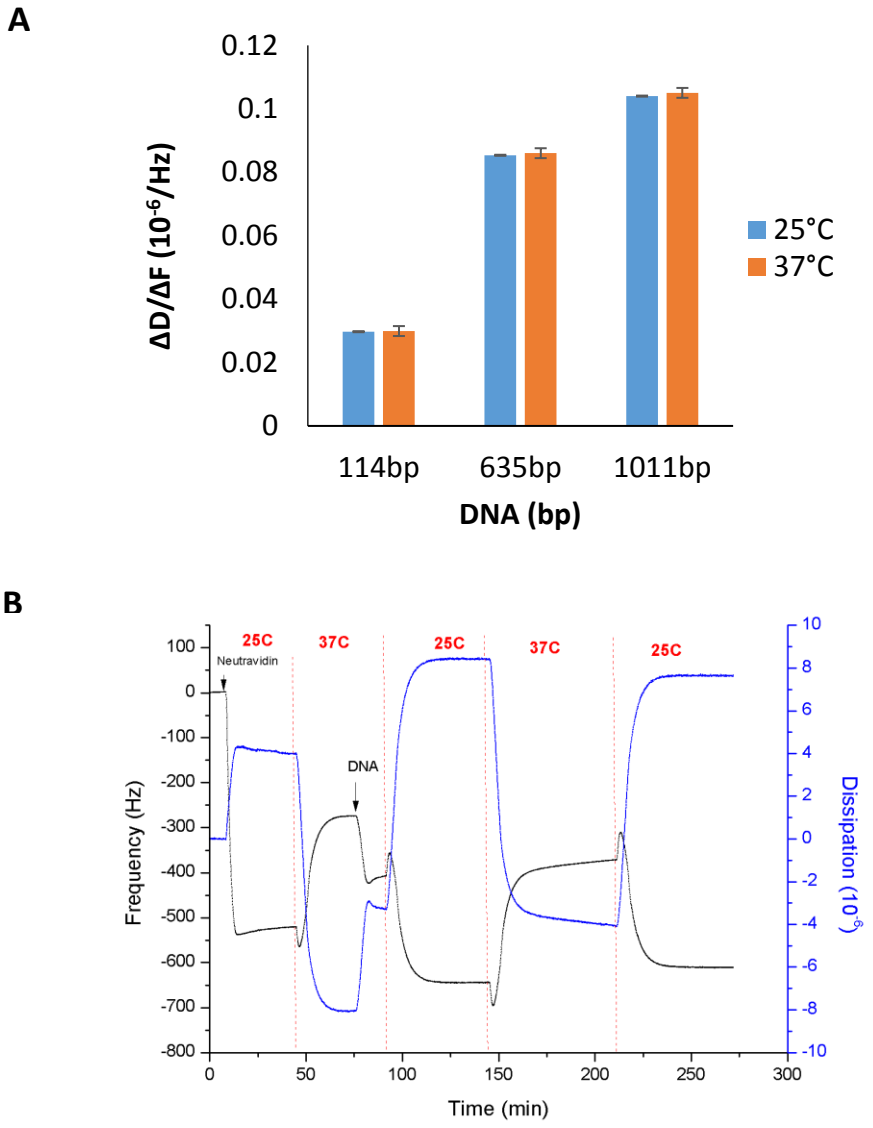

Figure 21: A) Diagram of the effect of changing temperatures on the acoustic ratio for three different DNA lengths and **B)** example of a QCM-D sensogram

Since equation 1 will be used to determine the elongation of the DNA molecules we wanted to compare the already published measurements with our experimental points. As can be seen from figure 22 red line (new DNA acoustic ratios) is above the black line (previously published data) (Tsortos et al, 2016). One possible explanation was the modification of the surface with neutravidin. During the experiments we observed that the ratio of neutravidin was higher than expected (~0.009 10^{-6}/Hz in contrast to ~0.004 10^{-6}/Hz). This means that this batch of neutravidin had a different organization on the surface. This was also confirmed by light scattering experiments which proved that there were a lot of aggregates of neutravidin (data not shown).

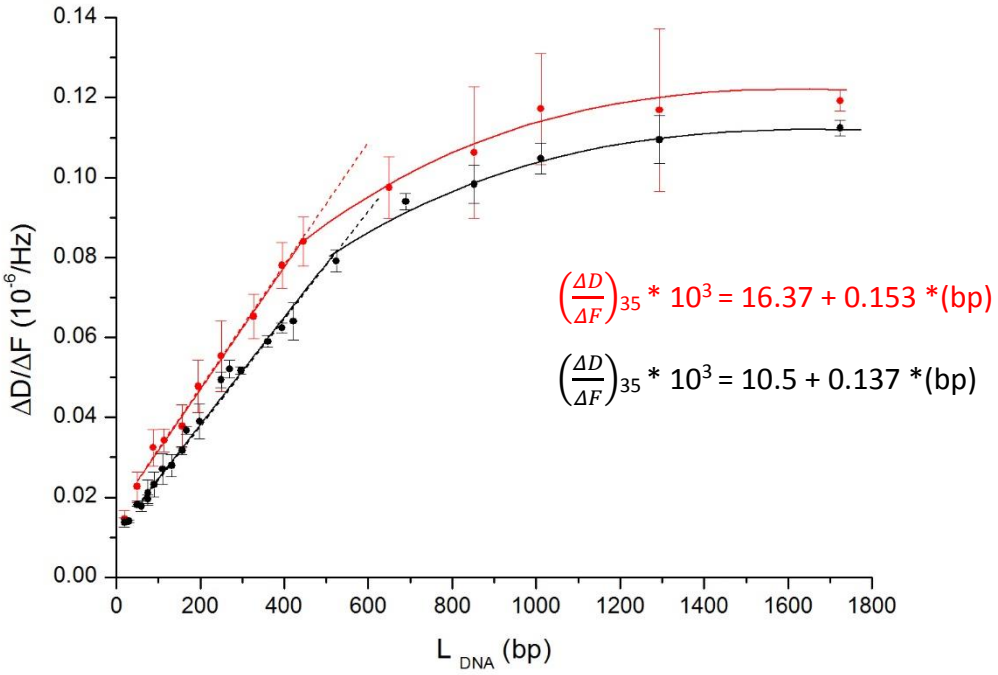

Figure 22: The relation between new experimental ΔD/ΔF values (red line) for linear dsDNA in the range of 20 to 1724bp compared to previously published acoustic ratio values (black line)

In this figure we observe that the linear relationship between length and ΔD/ΔF values up to a certain length is higher than predicted by equation 1 and that the plateau value here is ~ 0.12 (10^{-6}/Hz). The new equation derived from the linear part (up to 500bp) is:

$$\left(\frac{\Delta D}{\Delta F}\right)_{35} * 10^3 = 16.37 + 0.153 *(bp) \qquad \textbf{(Equation 2)}$$

In order to avoid this phenomenon we tested other possible substrates. Streptavidin (SAv) and Avidin (Av) have become widely used molecular tools in biotechnology thanks to their remarkable affinity for biotin. In contrast to NAv, both SAv and Av form dense, stable protein monolayers that retain biotin-binding activity and are largely inert to the unspecific binding of bovine serum albumin (Wolny et al, 2010). The adsorption

behavior of Av differed markedly from that of NAv. It reached a plateau at around 180.7 Hz, which is the half of the response for NAv and almost zero dissipation since it forms monolayer. Any gaps on the gold surface can be filled with BSA which we have previously checked that doesn`t bind biotinylated DNA (Figure 23).

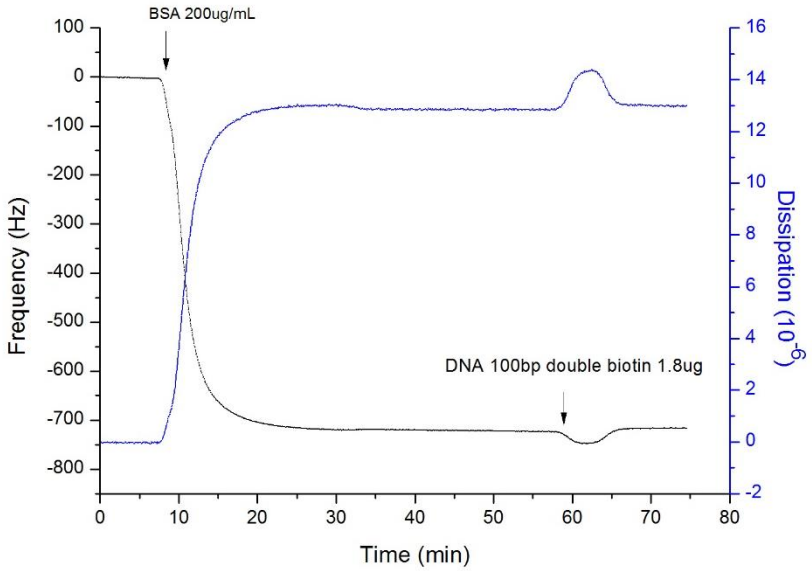

Figure 23: Non-binding of double-biotinylated DNA 100bp on BSA

The problem with avidin as a substrate was that since it has a pI around 9, in PBS buffer (pH: 7.4) it is positively charged. As a consequence "positive avidin" binds "negative DNA" not just from biotin but also from non-specific sites, giving us different acoustic ratio [[ΔD/ΔF (10^{-6}/Hz)] values each time (Figure 25.A, real data not shown).

Next, we investigated the adsorption of SAv to gold. The advantage of streptavidin is that it is negatively charged at PBS buffer since it has a pI around 5, so we can overpass the nonspecific binding of DNA (control experiments were done). According to Wolny`s publication (Wolny et al, 2010) absorption of SAv on gold surface should give around 210 ± 14 Hz. Unfortunately, we could only get around 80 Hz, which is by far different than what was expected. The holes that were on the surface were filled with BSA, so that the absorption of biotinylated DNA molecules on gold was prevented. However, the signal obtained after the addition of DNA molecules was not reproducible (Figure 25.B and C).

In our attempt to find the "perfect substrate" we tested the possibility of not having a substrate at all. Biotinylated DNA seems to bind on gold easily in contrast to non-biotinylated DNA (Figure24). The drawback of this process is that afterwards both intercalators interact with gold and the signal obtained couldn`t be explained somehow (Figure 25.D) (data not shown).

Thus we continued our experiments with NAv but equation **2** was used as a reference and not equation **1**.

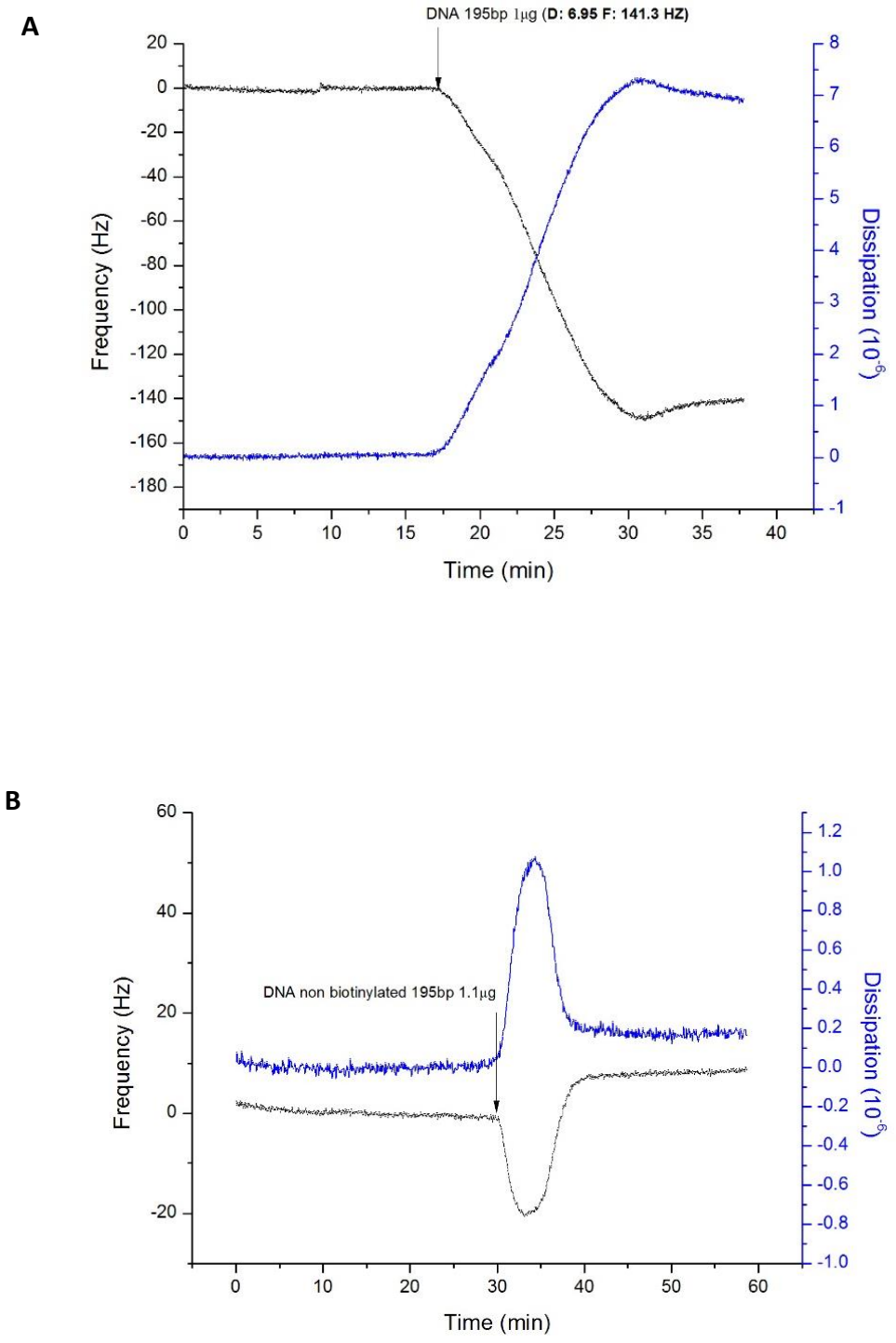

Figure 24: Sensogram of biotinylated DNA (**A**) and non-biotinylated DNA (**B**) absorption on gold

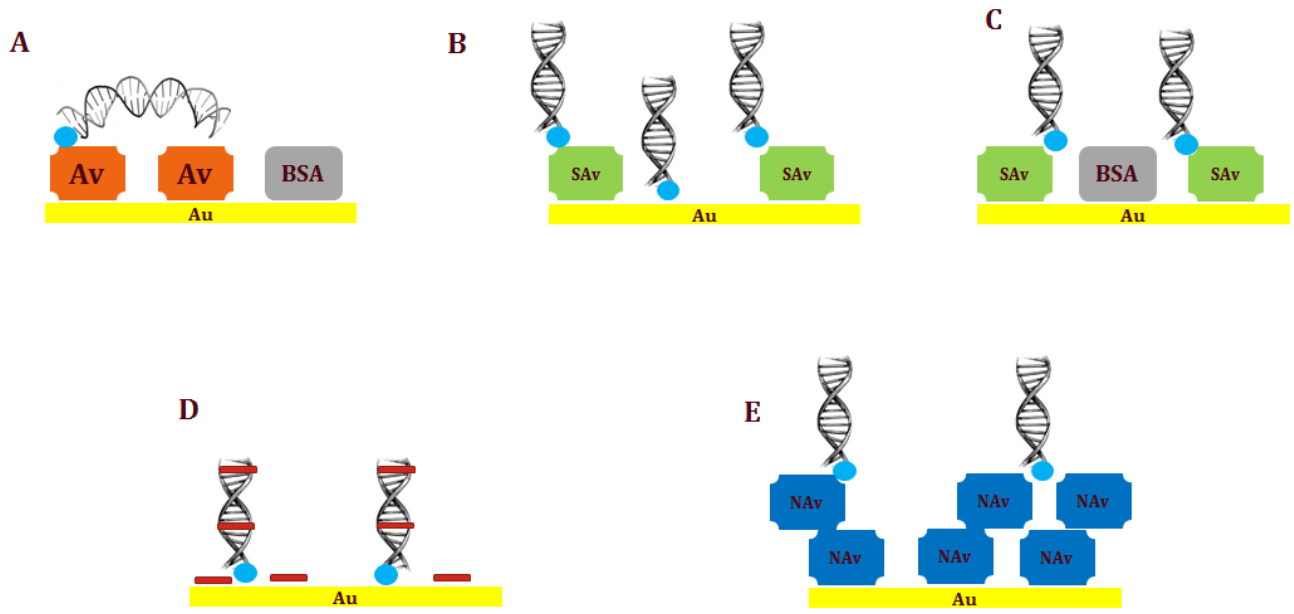

Figure 25: Different surface modifications. A) Avidin with biotinylated DNA on gold, B) Streptavidin with biotinylated DNA on gold, C) Streptavidin and BSA with biotinylated DNA on gold, D) biotinylated DNA on gold with ethidium bromide (red) and E) NetrAvidin multilayer with biotinylated DNA (not drawn to scale)

- **Ethidium Bromide**

The aim of this study was to investigate if the QCM-D technique could be used to characterize the conformational changes of DNA induced by external agents and more specific from intercalators. Firstly a titration curve of EtBr was obtained by the acoustic ratio (ΔD/ΔF) changes plotted against increasing concentrations of the intercalator for three different DNA lengths i.e. 114bp, 195bp, 327bp (Figure 27). Ethidium bromide was added in situ to the previously immobilized dsDNA molecules through biotin-NAv interactions. As figure 26 shows, EtBr has a clear effect on DNA, which is totally reversible after the buffer rinsing. More specific, there is an increase in the signal as a consequence of the elongation of the double helix after the addition of the ethidium molecules, which is well known from literature.

In order to avoid the dependence on the ratio of neutravidin, the elongation of the DNA molecules after the addition of the intercalator was quantitatively derived from the comparison between the ratio of the DNA-EtBr complex (after the subtraction of the negligible effect of the EtBr on neutravidin) and the DNA alone. Based on the theory that the acoustic ratio ΔD/ΔF is related to the base pairs of the DNA with a simple, linear equation (i.e. **$\Delta D/\Delta F * 10^3 = A * (bp) + B$**) three different types of analysis were made to ensure that the results obtained are independent to the treatment of the data.

In the first analysis, the acoustic ratio of the DNA was given from the changes in the frequency and dissipation, the number of base pairs of the DNA was known from the PCR reaction, the slope was kept constant using the equation **1** (i.e. 0.137) and for each set of experiment a new intercept was found as an inner control to the experiment. This "new" intercept was used in the equation of the elongated DNA in order to find the "new" number of base pairs and therefore the elongation from the comparison of the "new" with the initial ones $(\frac{\mathrm{bp}'}{\mathrm{bp}})$.

$$(\frac{\Delta \mathrm{D}}{\Delta \mathrm{F}}) = 0.137 * (\mathrm{bp}) + \mathrm{B}$$

$$\downarrow$$

$$\mathrm{B} = \left(\frac{\Delta \mathrm{D}}{\Delta \mathrm{F}}\right) - 0.137 * (\mathrm{bp}) \quad \textbf{(Equation 3)}$$

However:

$$\left(\frac{\Delta \mathrm{D}}{\Delta \mathrm{F}}\right)' = 0.137 * (\mathrm{bp}') + \mathrm{B}$$

$$\downarrow$$

$$(\mathrm{bp}') = \frac{\left(\frac{\Delta D}{\Delta F}\right)' - \mathrm{B}}{0.137}$$

$$\downarrow \textbf{(3)}$$

$$(\mathrm{bp}') = \frac{\left(\frac{\Delta \mathrm{D}}{\Delta \mathrm{F}}\right)' - \left(\frac{\Delta \mathrm{D}}{\Delta \mathrm{F}}\right) + 0.137 * (\mathrm{bp})}{0.137} \quad \textbf{(Equation 4)}$$

Knowing the (bp') the elongation is given as $(\frac{\mathrm{bp}'}{\mathrm{bp}})$.

The second analysis was the same with the first one, but the slope used derived from the equation **2** (i.e. 0.153). Finally, the last analysis was dependent on the intercept (i.e. 16.37) of the equation **2** and not on the slope. Meaning:

$$\frac{\mathrm{bp}'}{\mathrm{bp}} = \frac{\left(\frac{\Delta \mathrm{D}}{\Delta \mathrm{F}}\right)' - 16.37}{\left(\frac{\Delta \mathrm{D}}{\Delta \mathrm{F}}\right) - 16.37}$$

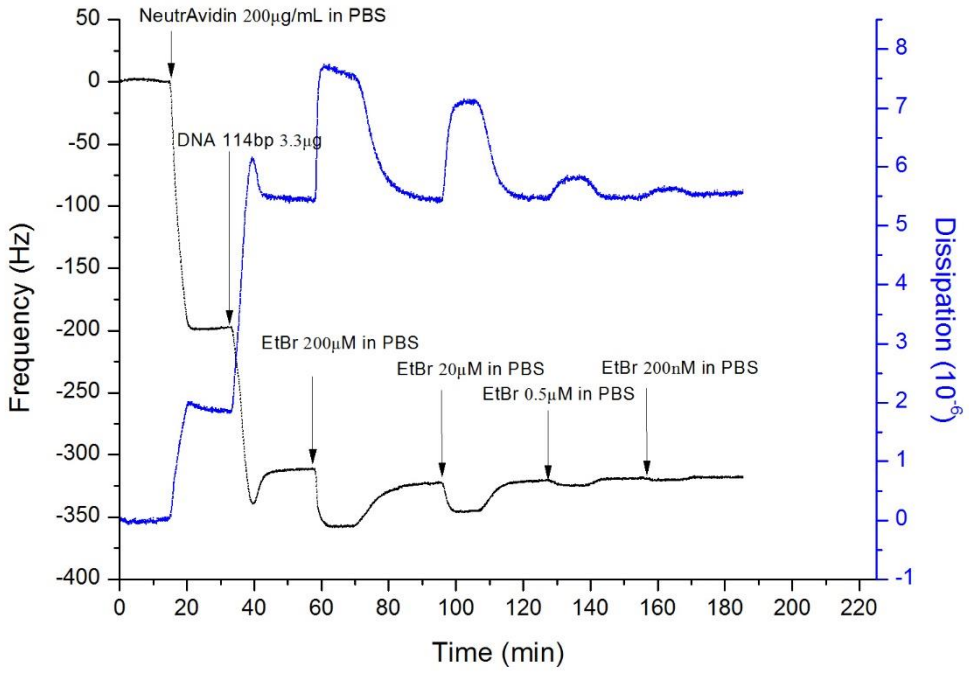

Figure 26: A QCM-D sensogram for the addition of four different concentrations of EtBr (200µM, 20µM, 0,5µM and 200nM) on dsDNA 114bp.

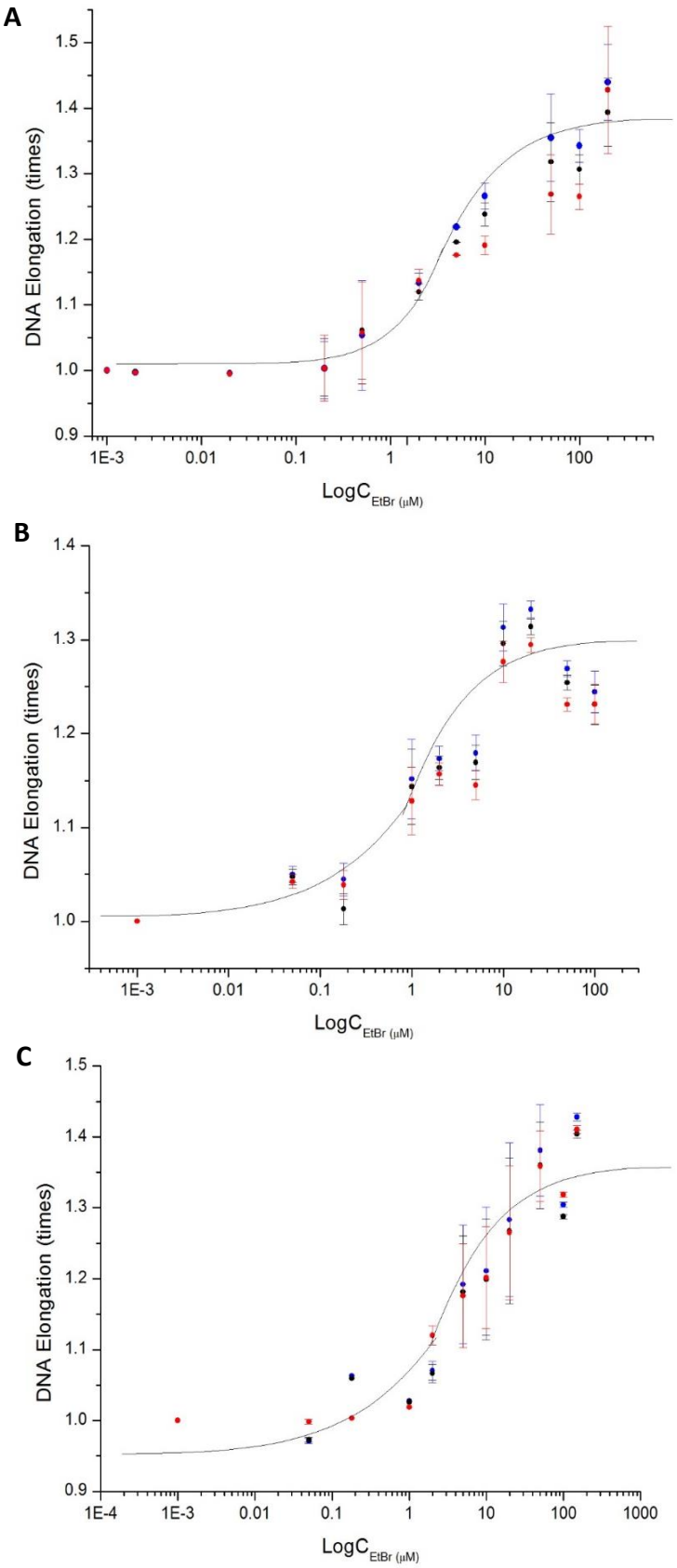

Figure 27: Titration curve of EtBr on dsDNA **A)** 114bp, **B)** 195bp and **C)** 327bp showing the different types of analysis. Blue points derived from analysis 1, black points derived from analysis 2 and red points from analysis 3.

The results from the plots above indicate that the maximum elongation that can be detected by QCM-D is 1.4 times longer than the DNA molecule alone and this is independent of the length of dsDNA. Also, a good signal can be obtained from a concentration starting at least from 0.5μM EtBr and reaches a plateau at 20μM. Thus, DNA molecules of a variety of lengths were incubated with a concentration of EtBr which gives the maximum elongation (i.e. 100μM) in order to check the difference in the acoustic ratios. All the control experiments were taken into consideration and no difference was observed between pre-incubation of the intercalator with the dsDNA and addition of the intercalator in real time to the QCM-D.

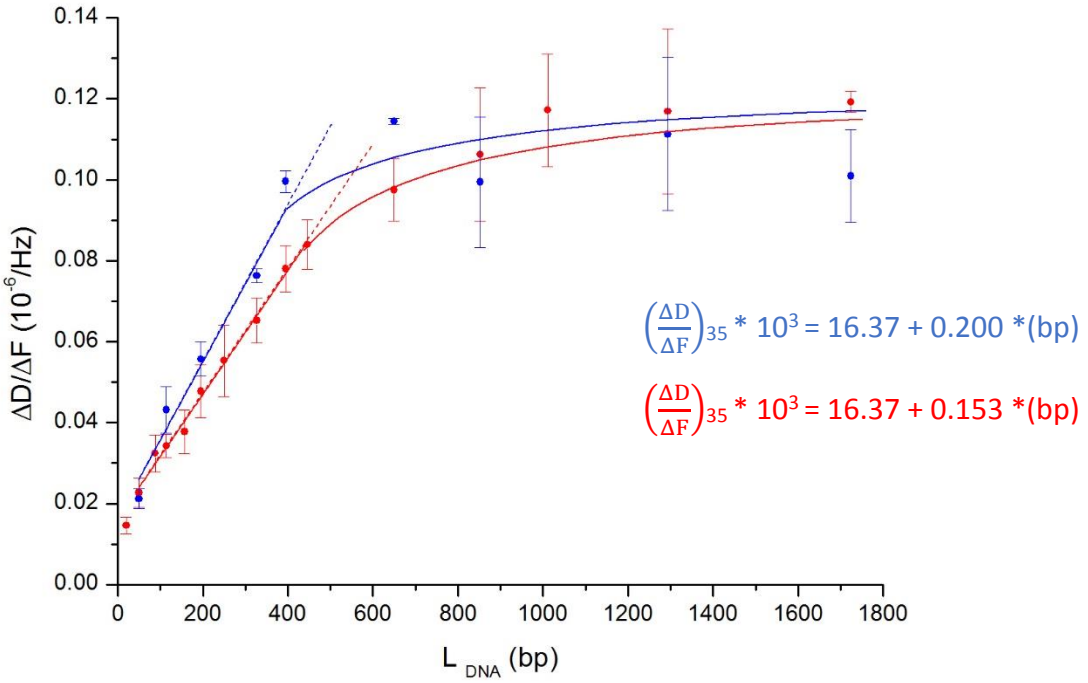

Figure 28: The acoustic ratio (ΔD/ΔF) obtained after the effect of 100μM EtBr on DNA versus number of base pairs of DNA (blue points), compared with the acoustic ratio values of DNA from figure 19 (red and black points).

As figure 28 indicates, the ratios of the DNA molecules in the presence of ethidium bromide is clearly higher than the ratios of the DNA molecules alone. The equation derived from the first part of the blue line is:

$$\left(\frac{\Delta D}{\Delta F}\right)_{35} * 10^3 = 16.37 + 0.200 *(bp) \qquad \textbf{(Equation 5)}$$

Due to the phenomenon of neutravidin forming aggregates, this new line cannot be compared to the initial line (black line-equation 1). This is the reason why the intercept was kept fixed at 16.37, which derived from equation 2. The difference in the slopes of the two lines indicate the elongation of the DNA molecules which is 1.31 times.

UV-Vis Absorption

Another method for detection of DNA–drug interactions is UV-Vis absorption spectroscopy through measuring the changes in the absorption properties of the drug or the DNA molecules. Thus, we started our experiments checking this technique the same way as Peacocke & Skerrett (Peacocke et al, 1956) for the interaction of proflavine with nucleic acids. The treatment of the results was made in accordance to Peacocke & Skerrett analysis (Peacocke et al, 1956) and Scatchard (Scatchard, 1949) as described in the Introduction. The concentrations used were 100μM ethidium bromide and 700μM lambda DNA calculated in bp. As figure 29 demonstrates ethidium bromide exhibits maximum absorbance at 480nm when it is free but when it is bound to nucleic acids at 520nm. The isosbestic point seems to be around 515nm.

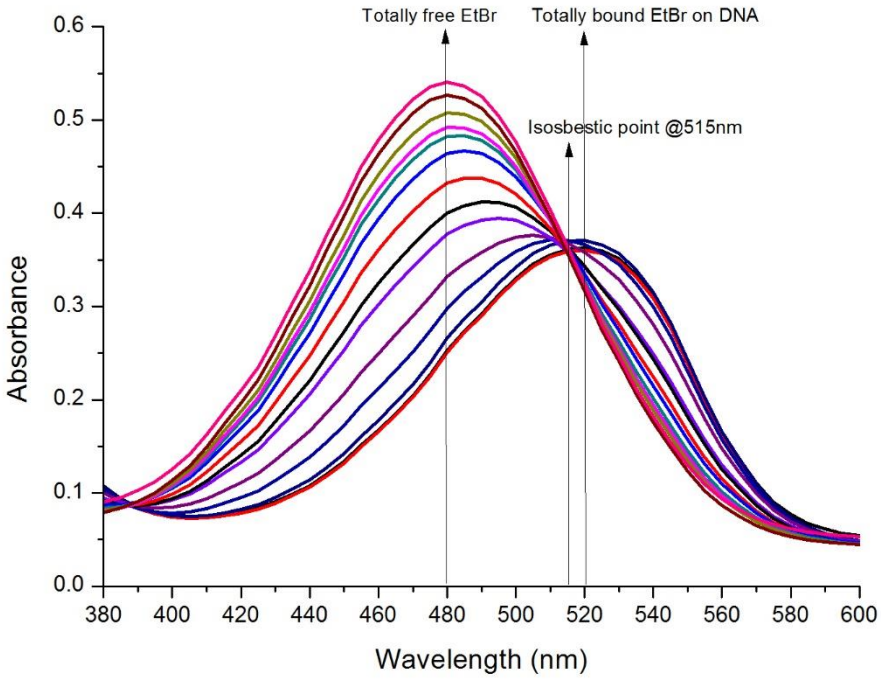

Figure 29: Effect of nucleic acids on the absorption spectrum of ethidium bromide.

Figure 30 shows the analysis of the data obtained from the above graph according to the equations discussed in the Introduction. Keeping only the linear parts of the plot C/r versus C we can obtain the values $K_a = 0.13 \times 10^6\ M^{-1}$ and $N_{bp} = 2.7$.

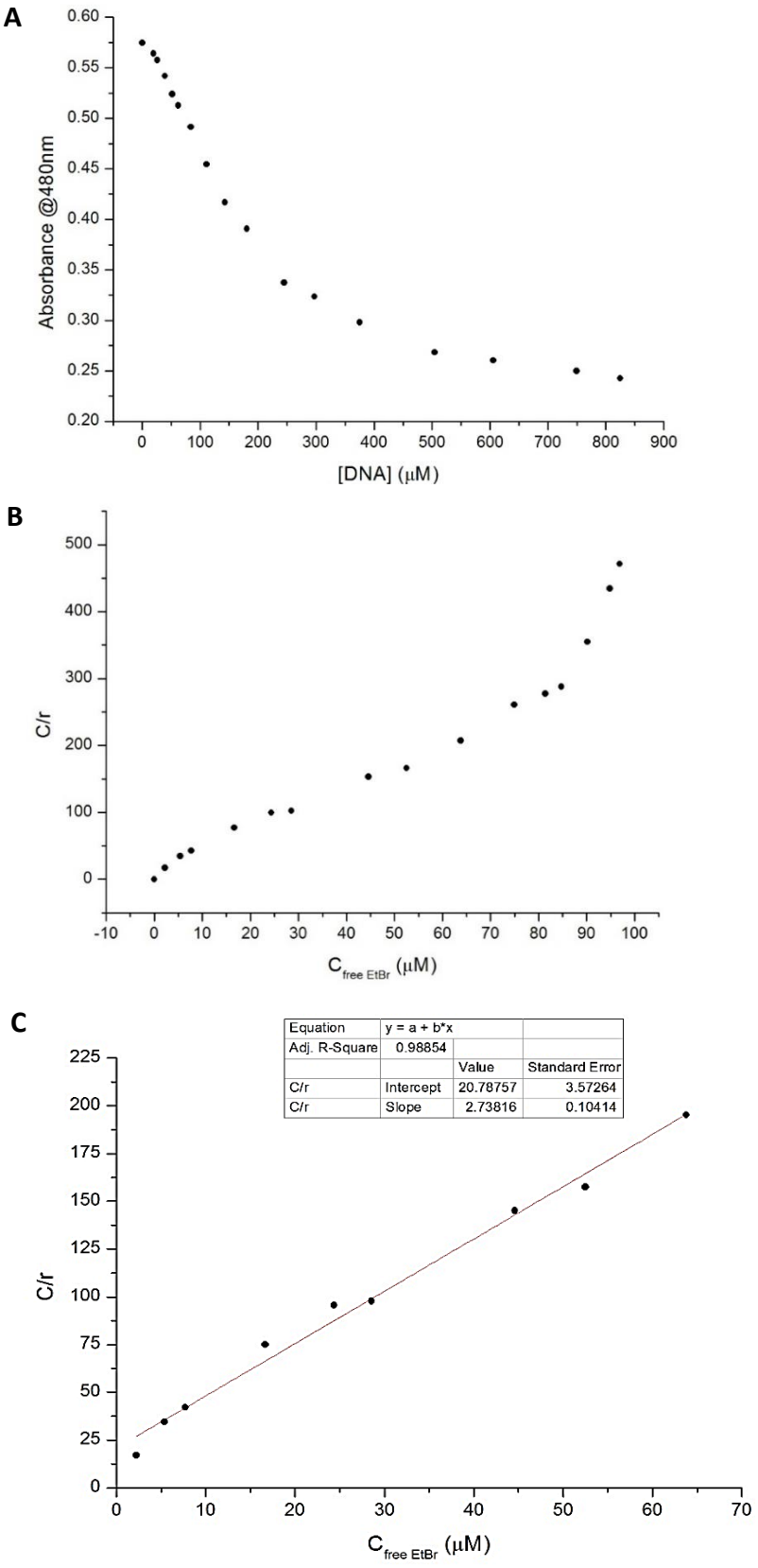

Figure 30: Binding of ethidium bromide to lambda DNA. **A)** Plot of Absorbance @480nm versus the concentration of the DNA calculated in bp. **B)** The total plot of C/r versus C and **C)** The linear part of the plot C/r versus C

The same experiment was performed with a smaller DNA molecule (327bp) made by PCR reaction. As figure 31 shows the values obtained here were $K_a = 0.55 \times 10^6\ M^{-1}$ and $N_{bp} = 1.61$.

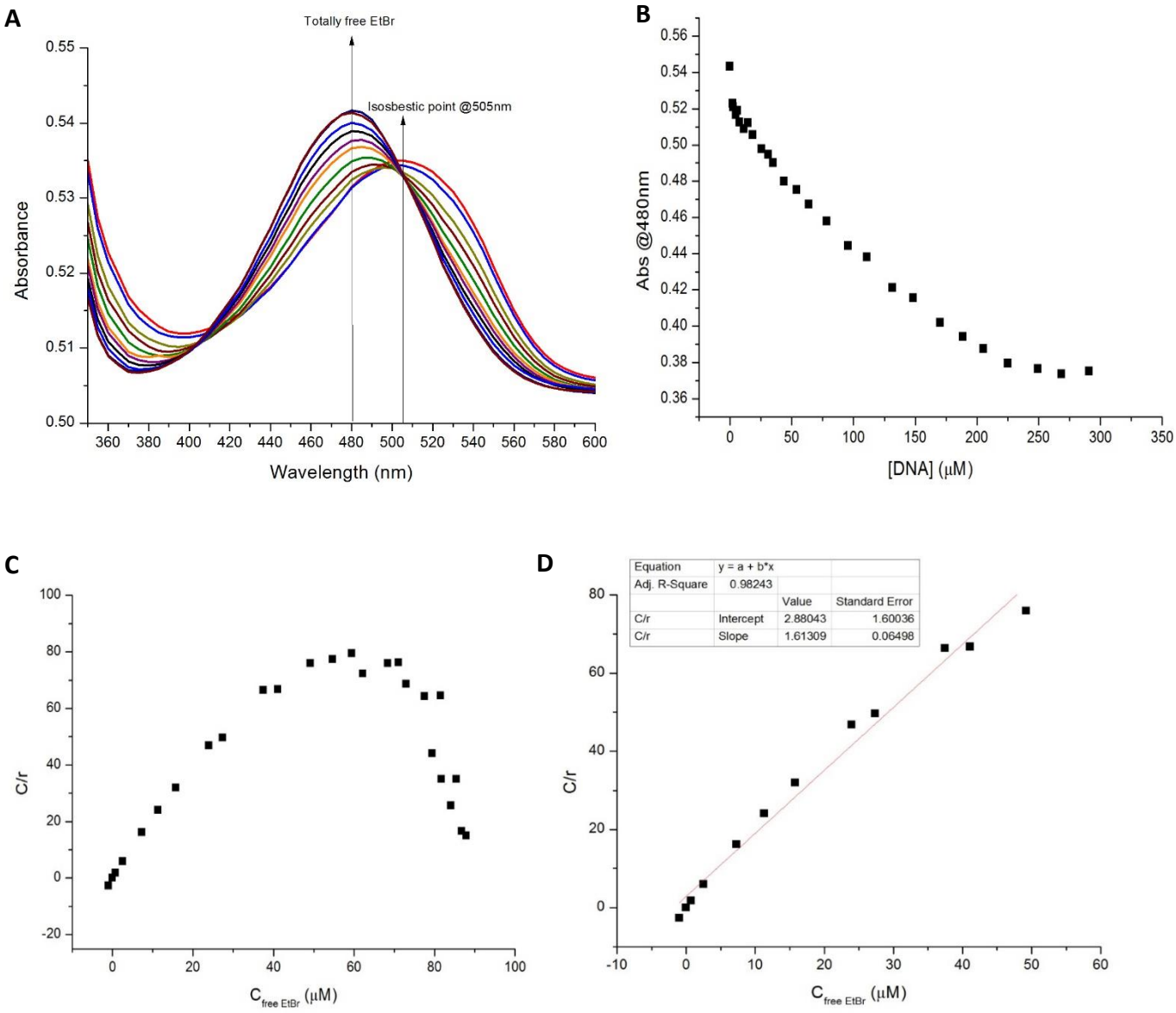

Figure 31: Binding of ethidium bromide to dsDNA 327bp. **A)** Effect of nucleic acids on the absorption spectrum of ethidium bromide **B)** Plot of Absorbance @480nm versus the concentration of the DNA calculated in bp. **C)** The total plot of C/r versus C and **D)** The linear part of the plot C/r versus C

AFM experiments

Atomic force microscopy (AFM) was used as a last method to verify our results. AFM is a very versatile and powerful microscopy technology for studying samples at nanoscale. It is versatile because an atomic force microscope can not only image in three-dimensional topography, but it also provides various types of surface measurements to the needs of scientists and engineers. In our case dsDNA molecules 635bp long were scanned by AFM and compared with the same dsDNA molecules treated with 100µM EtBr (Figure 32).

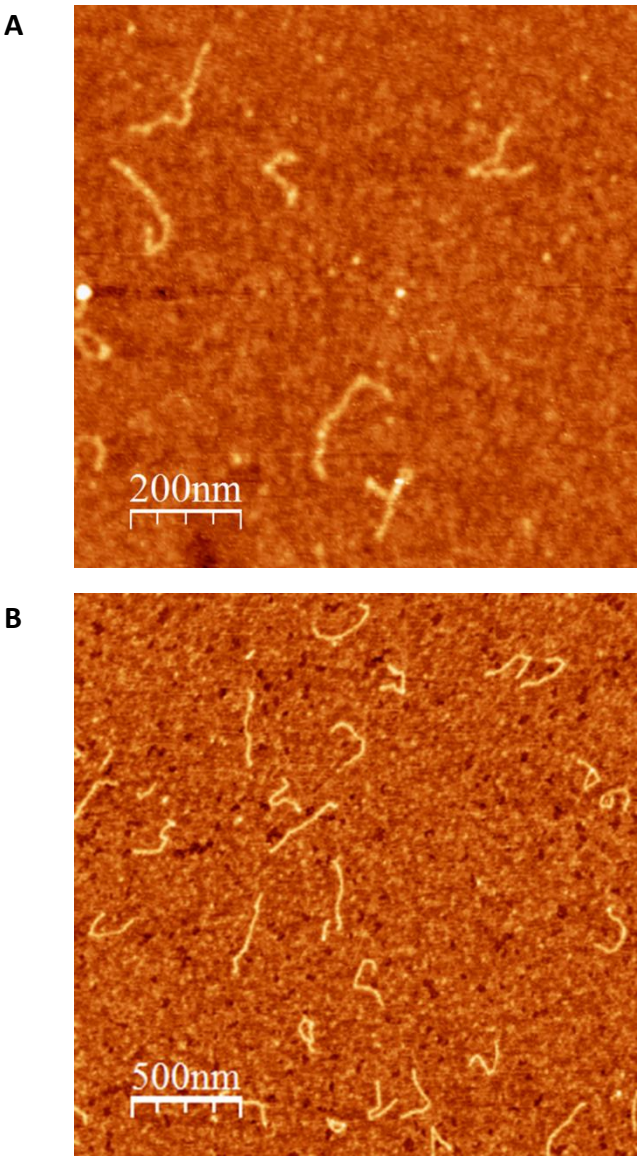

Figure 32: AFM images of dsDNA molecules **A)** 635bp in Tris buffer 10mM plus 9mM $MgCl_2$ (256 pixels 1µm x 1µm) and **B)** 635bp + 100µM EtBr in Tris buffer 10mM plus 9mM $MgCl_2$ (512 pixels 2.5µm x 2.5µm)

After the analysis of these images we obtained the two following histograms. As figure 33 indicates dsDNA molecules not treated with EtBr are around 240.2 ± 26.5nm long, which is 11% different from the general accepted 215.9nm (i.e. 0.34nm per bp). After the treatment with 100µM EtBr the same molecules seems to be elongated to 320.6 ± 39.5nm long. This elongation is 1.33 times the initial length of the DNA, which in accordance to our previous results with the QCM-D.

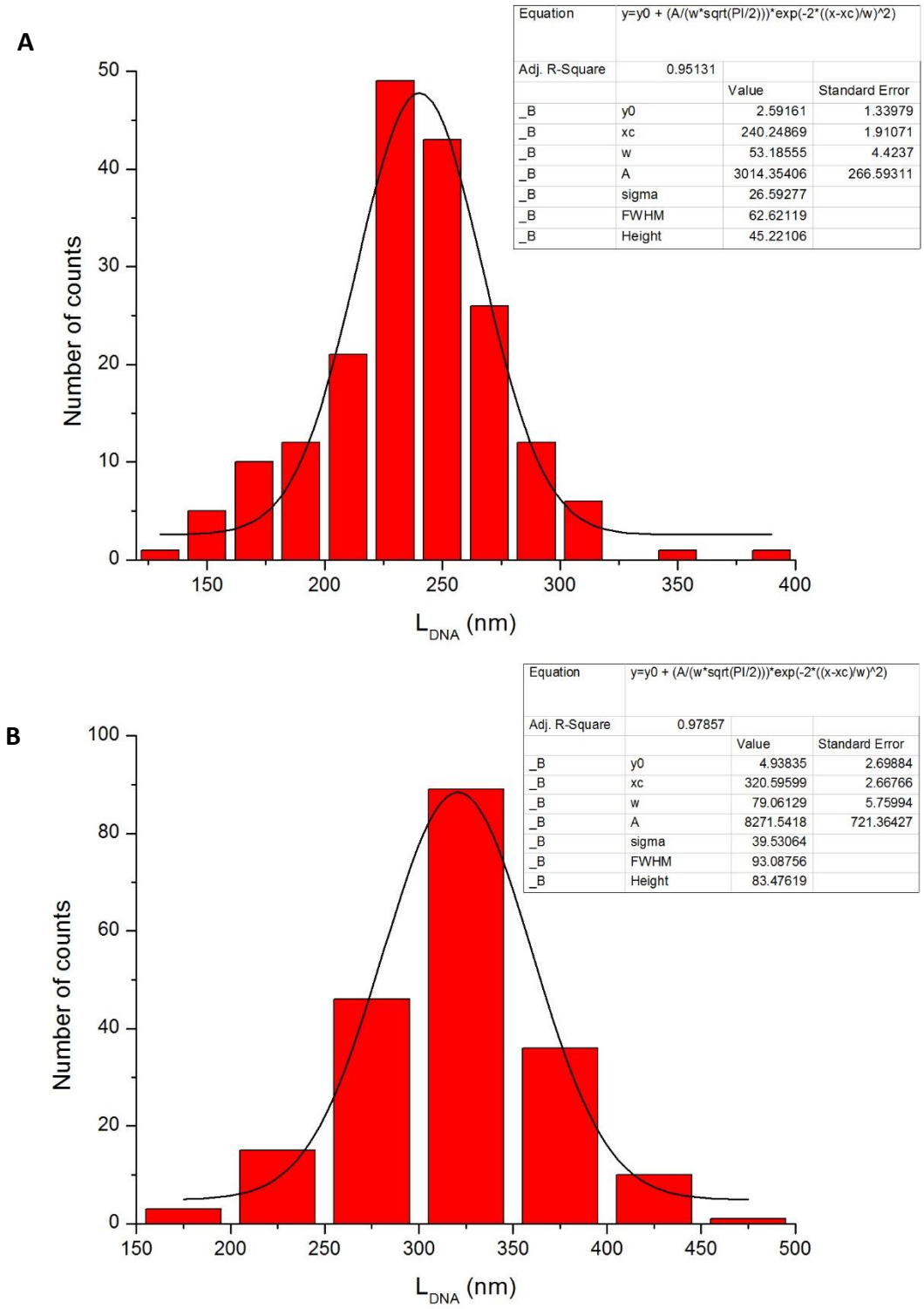

Figure 33: Histograms obtained from AFM images **A)** dsDNA 635bp and **B)** dsDNA 635bp + 100µM EtBr

- **GelRed**

In the final part of this work, we tested the bis-intercalating agent, GelRed. At the beginning of our experiments we wanted to check whether we could get a titration curve the same way as with EtBr. The problem with these experiments was that when we increased the concentration of GelRed on DNA (starting from 20μM and above), we observed a decrease in the frequency and the dissipation signal (Figure 34). This is probably explained due to the fact that bifunctional intercalators are able to insert to DNA molecule in two different ways: through intramolecular and intremolecular cross linking depending on the number of DNA molecules that interact with the bifunctional intercalator (Figure 9) (Aleksic et al, 2014).

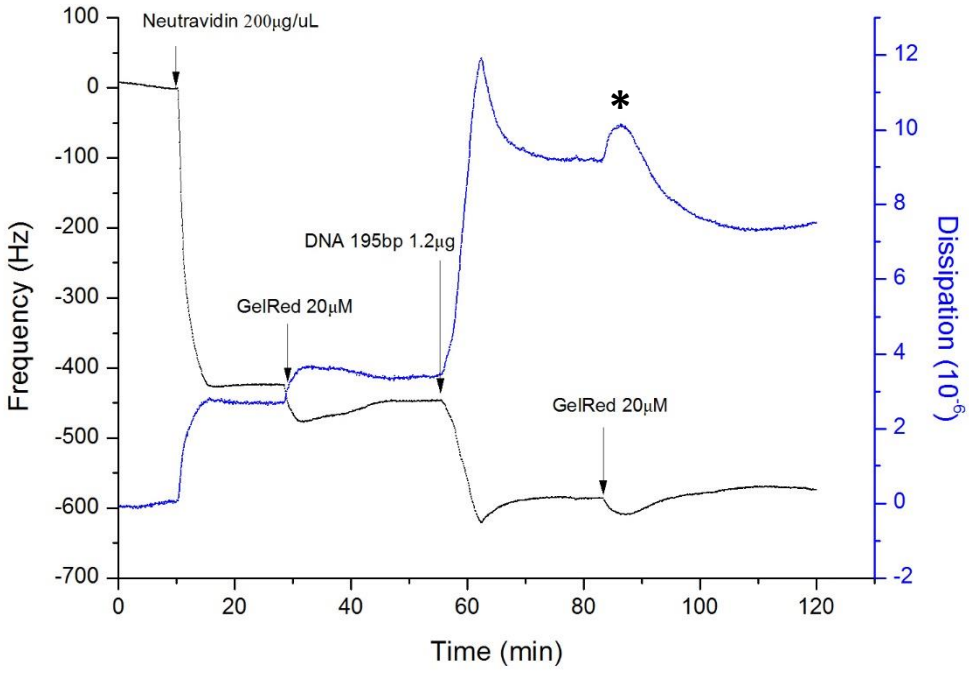

Figure 34: An example QCM-D sensogram of the effect of GelRed 20μM on DNA 195bp. *indicates the decrease in the frequency and the dissipation signal for concentrations of GelRed above 20μM

Another main difference between EtBr and GelRed that can be easily observed (Figure 35) was that the binding of GelRed to DNA is partially irreversible which means that most of the molecules of the intercalator are strongly bound to the DNA helix and stay attached to it, even after the washing step (Figure 35). This phenomenon is in contrast to the behavior of EtBr but in accordance to the properties of the structure of GelRed, thus the DNA-GelRed complex is much more stable than the DNA-EtBr complex.

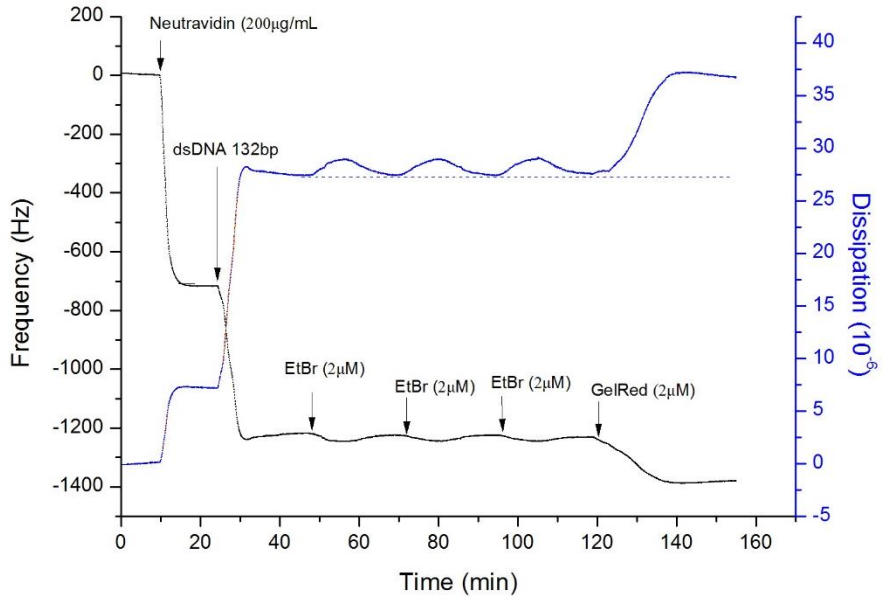

Figure 35: An example QCM-D sensogram of the effect of EtBr (2µM) and GelRed (2µM) on DNA 132bp

Therefore we tested it spectrophotometrically with the exact same way as for ethidium bromide (Figure 36). The concentration used of GelRed was the half of what was used for ethidium, i.e. 50µM and the extinction coefficient used was the double, i.e. 11200 at 480nm when it was totally free.

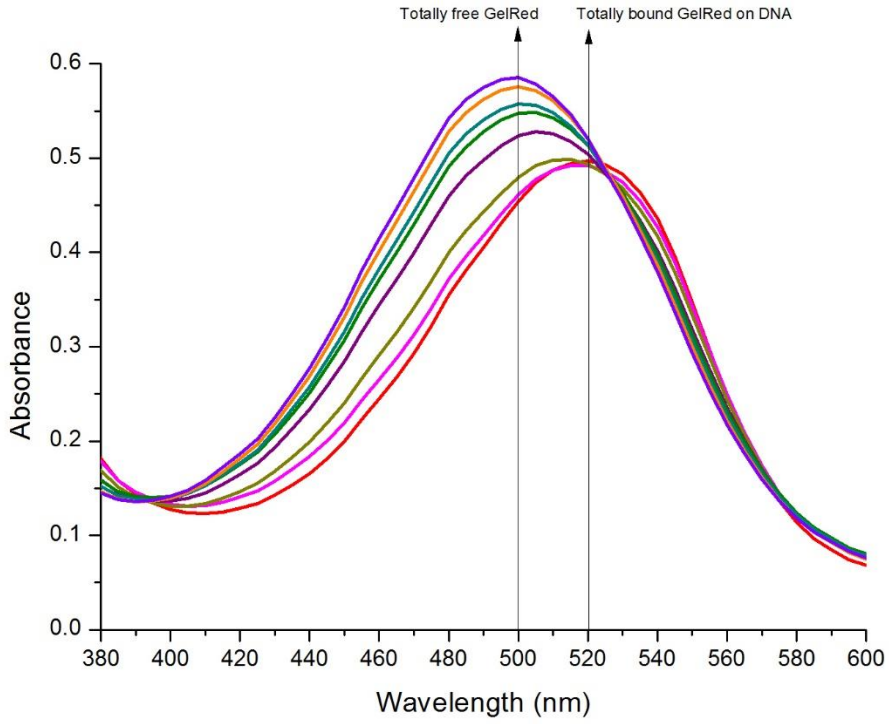

Figure 36: Effect of nucleic acids (lambda DNA) on the absorption spectrum of GelRed

Figure 37 shows the analysis of the data obtained from the above graph according to the equations discussed in the introduction. Taking only the linear part of plot C/r versus C into consideration, K_a is equal to 2.3 x 10^6 M^{-1} and N_{bp} = 4.4.

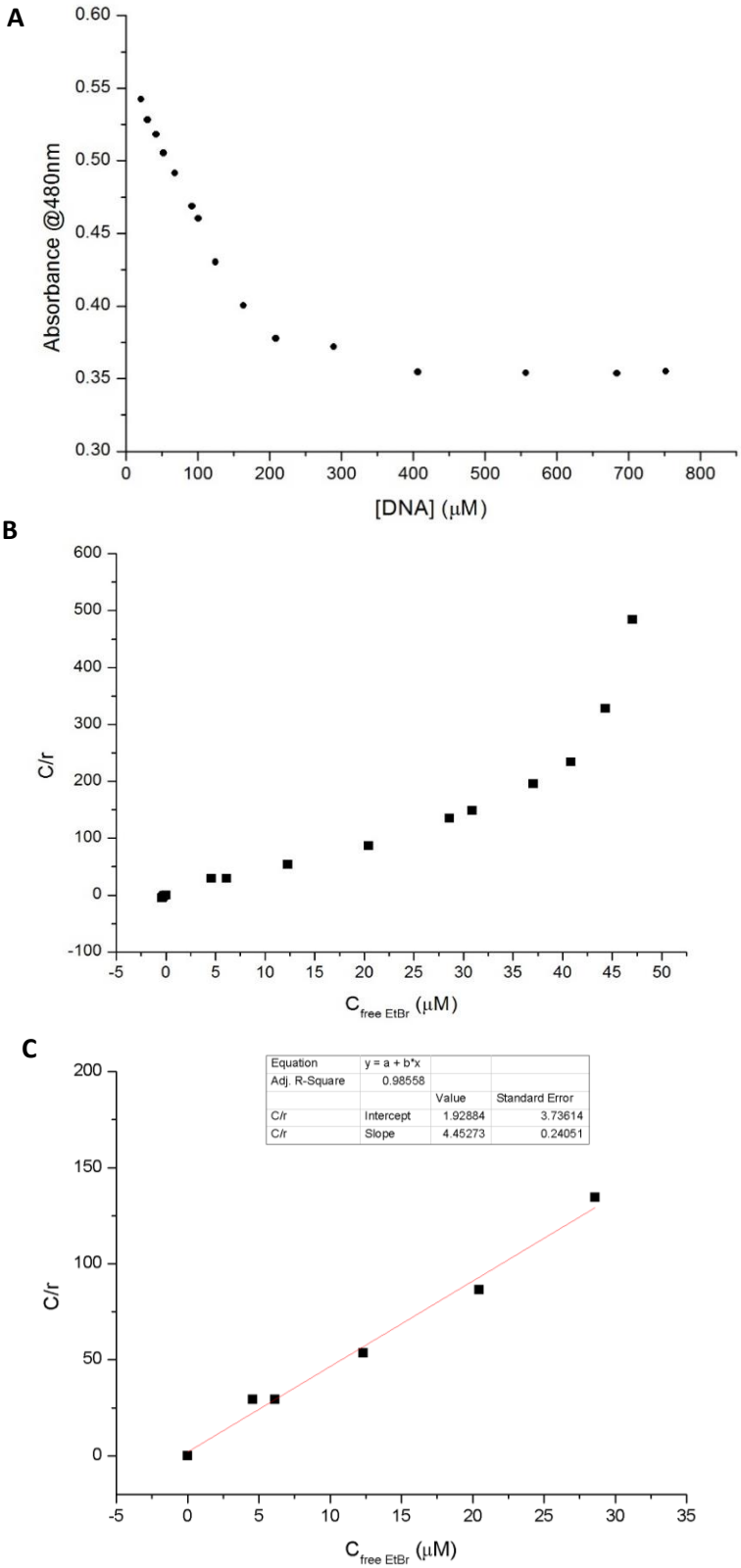

Figure 37: Binding of GelRed to lambda DNA. **A)** Plot of Absorbance @480nm versus the concentration of the DNA calculated in bp. **B)** The total plot of C/r versus C and **C)** The linear part of the plot C/r versus C

Finally, through some preliminary experiments with QCM-D, a competitive equilibrium has been observed between GelRed and EtBr for the binding on dsDNA. DNA molecules were immobilized on gold surfaces through biotin-neutravidin interactions. GelRed 2µM in PBS was added in situ on the surface and stayed attached to the DNA even after the buffer rinsing. As Figures 38 and 39 shows when EtBr was added afterwards on the same surface, a partial removal of the GelRed from the DNA was detected.

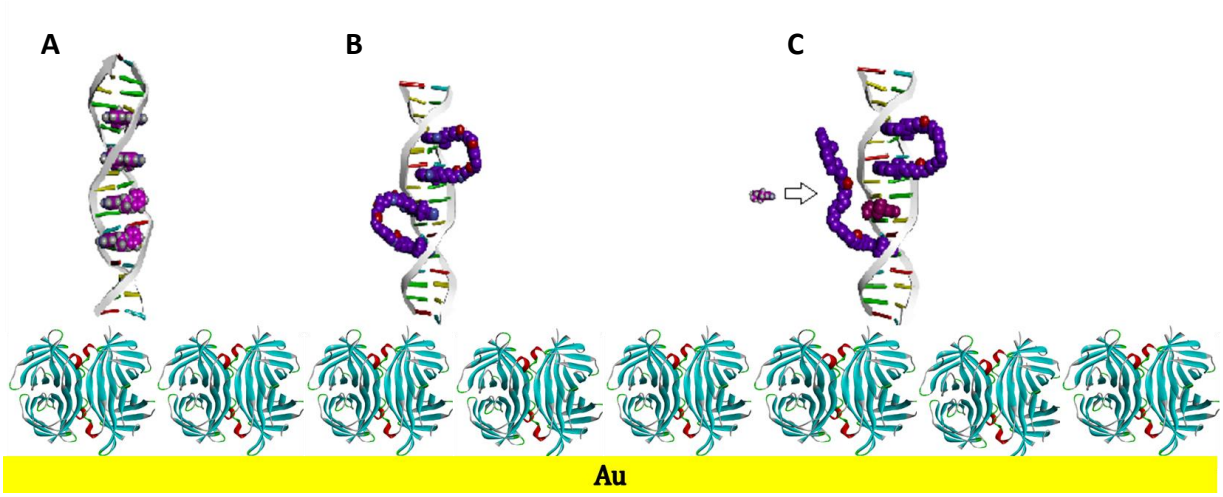

Figure 38: A representation of the DNA-intercalators complexes immobilized to the gold surface through the biotin- NAv (blue molecule) interactions**. A)** DNA-EtBr (purple) complex**, B)** DNA-GelRed (dark purple) complex and **C)** GelRed removal from the DNA-GelRed complex from EtBr molecules (not drawn to scale)

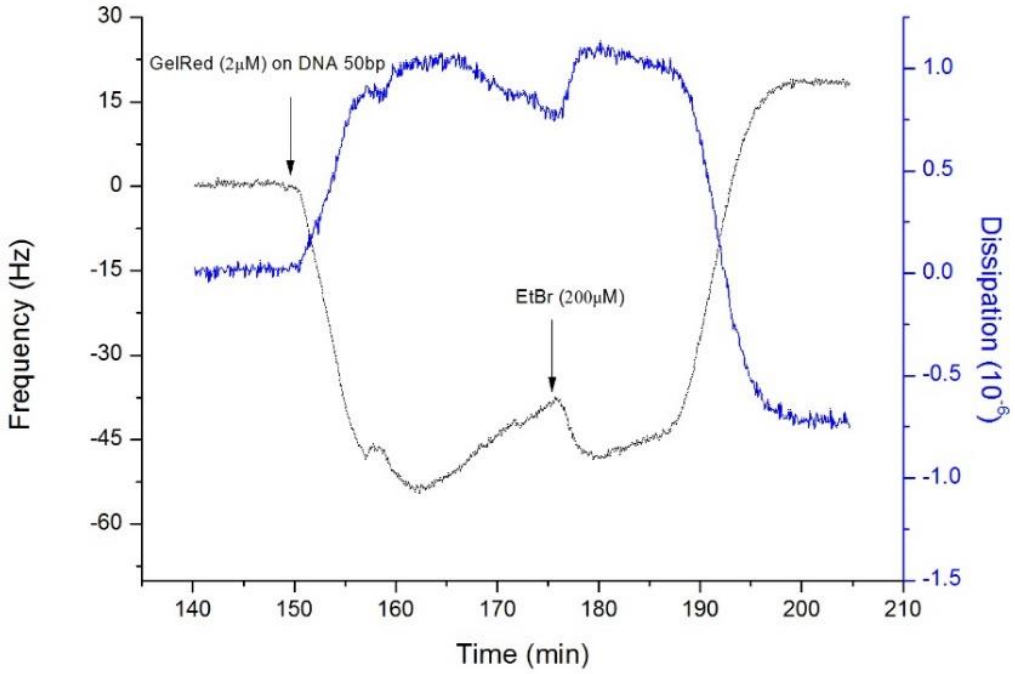

Figure 39: An example QCM-D sensogram of the removal of GelRed (2µM) from dsDNA 50bp by 200µM EtBr

DISCUSSION

Small molecules interact with nucleic acids through various covalent and noncovalent interactions and interrupt their natural biological functions. Intercalation of molecules to nucleic acids is a unique noncovalent interaction where a small planar aromatic moiety is inserted between the adjacent base pairs of DNA. This type of interaction generally causes stabilization, local unwinding, lengthening and some other structural changes in the DNA. However the intercalators are often used as drugs in cancer treatment, but also as antimicrobial or antiparasitic agents. Moreover, intercalating agents are also used as probes to study the structure and dynamics of nucleic acids.

Due to the special binding mode and specific properties of the intercalators, intercalation is possible to be characterized by various biophysical methods. The methods can be divided into two categories: **(1)** methods which characterize the interaction, either qualitatively or quantitatively, but by themselves provide little information on the mechanism of the binding, or **(2)** methods that address directly on the physical changes in DNA associated with intercalation i.e. orientation of the bound dyes, unwinding of closed circular DNA and extension of the double helix. In this study, we wanted to monitor the conformational changes in DNA of various lengths, after the binding of mono- and bis-intercalator agents using both types of methods. Our choice of Ethidium Bromide (EtBr) as a mono-intercalating agent was due to the large literature pertaining to the physical and biochemical properties of this dye. On the other hand, the bis-intercalator GelRed was chosen since no study has focused on the interaction of GelRed with DNA using the acoustic biosensor QCM-D up to today. Below, we give a more detailed view of the analyzed above results.

Surface modifications and experimental conditions

The importance of a well modified and well-structured surface has been reviewed a lot over the past years. For the immobilization of DNA molecules on gold surfaces a widely accepted way is through biotin- avidin interactions. Avidin and streptavidin did not meet the requirements of a nice substrate since avidin binds dsDNA molecules non-specific and streptavidin did not form a proper monolayer. On the other hand, neutravidin tended to form aggregates making the surface rougher than expected. This resulted in a higher energy dissipation after the binding of the dsDNA molecules and therefore in a higher and non-reproducible acoustic ratio. Equation 2 was created in respect to this phenomenon. It was observed that the linear relationship between length of DNA and acoustic values was kept up to a certain length and that the plateau value in this case is ~ 0.12 (10^{-6}/Hz). We observed from figure 22 that the two lines from equation 1 & 2 are not exactly parallel as expected but equation 2 seems to have a slightly higher slope. One possible explanation could come from the fact that equation 2 derived from acoustic ratios of neutravidin ranging from 0.005 (10^{-6}/Hz) to

0.009 (10^{-6}/Hz), compared to a much more narrow range of neutravidin ratios from equation 1 (from 0.004 to 0.005 10^{-6}/Hz).

Regarding the conditions in which all the experiments were carried out, it was found that no difference in the absorption and conformation of the molecules was noticed in a temperature higher than 25°C, i.e. 37°C. All the other conditions including the flow rate, the buffer, the concentrations used, the method of surface cleaning etc. were kept as used by biosensors laboratories.

UV-Vis absorption experiments for Ethidium bromide and GelRed

UV-Vis absorption spectra was chosen as a method type 1, meaning a method that does not characterize the mechanism of binding itself, but only the interaction, either qualitatively or quantitatively. Useful information can be obtained from a careful interpretation of the Scatchard plot of the binding parameters. All of this serves to emphasize, as originally stated by Waring and his colleagues that 1 molecule of ethidium bromide binds per 2-2.5 base pairs of DNA (Table 1). We kept the experimental setup and the treatment of the results in accordance to Peacocke & Skerrett (Peacocke et al, 1956) and Scatchard (Scatchard, 1949) and we obtained the values $K_a = 7.7 \times 10^6\ M^{-1}$ and $n_{bp} = 2.7$ for lambda DNA. The number of binding sites of EtBr is in agreement with the literature, but the observed association rate constant (K_a) is several orders of magnitude higher than expected. Nevertheless, there is a wide variation of the binding constants of ethidium bromide already in literature and these constants cannot be calculated precisely.

The same experiment was performed also with dsDNA 327bp made by PCR reaction. The values obtained after the analysis were $K_a = 1.79 \times 10^6\ M^{-1}$ and $n_{bp} = 1.61$. Here the binding constant agrees with the literature but the n_{bp} is not correct. This cannot be explained somehow. It is important to notice also here that in an experimental situation the Scatchard plot is often curved when r is moderately large. Thus the value of n is obtained by extrapolation of the linear region of the plots C/r versus C (Figures 30.B, 31C and 37.B). This can be attributed to a binding overlap effect (meaning that interactions between drugs could favor the binding of additional drugs or discourage further binding) or to the existence of more than one type of binding, resulting in more than one bound species (Dougherty et al, 1982).

Interestingly, the bis-intercalator GelRed was also tested spectrophotometrically and after the analysis of the data obtained gave us $K_a = 0.4 \times 10^7\ M^{-1}$ and $n_{bp} = 4.4$. These values are compatible with results expected for bis-intercalating molecules (Gaugain et al, 1978; Glazer et al, 1990; Berge et al, 2002; Gunther et al, 2010) but also with Crisafuli and his colleagues who found that each bound GelRed molecule effectively occupies 3.7 DNA base-pairs, increases the contour length by 0.65nm and binds strongly to DNA ($K_a = 10^7\ M^{-1}$) (Crisafuli et al, 2015).They are also in agreement with the observation that the binding of GelRed to DNA molecules is stronger than ethidium bromide (Figure 35).

Acoustics - AFM experiments

The relationship between the acoustic ratio of a surface attached biomolecule and its length (bp) in solution is valid but depends on the linker (i.e. Neutravidin). The validity is shown for a large range of synthetic DNAs of various sizes (20 - 1700 base pairs). There exists a question as to how easily measured can be the elongation of the DNA molecules when going from buffer to interaction with an intercalator. The results from the titration curves of ethidium bromide on dsDNA indicate that the maximum elongation that can be detected with the use of QCM-D is 1.4 which corresponds to n=2.5bp and that this elongation is independent of the length of dsDNA (Figure 27). The explanation can easily be given with an example, a 100bp DNA molecule after the 1.4 times elongation will become 140bp long. These theoretical “extra” 40bp can fit to the 100bp DNA only every 2,5bp which agrees with the bibliography (see Table 1). Also, noticing the titration curve of ethidium bromide, a good signal can be easily obtained from a concentration starting at least from 0.5μM EtBr and reaches a plateau at 20μM. This titration curve could not be made for GelRed. A logical explanation is that bis-intercalators are able to insert to DNA molecules in two different ways: through intramolecular and intermolecular cross linking depending on the number of DNA molecules that interact with the bifunctional intercalator (Figure 9) (Aleksic et al, 2014). This can lead to bending of the DNA molecules and therefore different acoustic ratio values.

Thus, checking a variety of lengths of DNA molecules with a plateau concentration of EtBr has a clear effect on the acoustic ratio but maintains the linear relation between length and acoustic values up to a certain length. Another important observation was that ethidium bromide can get easily removed from its complexed form in contrast to GelRed in which the binding to DNA is partially irreversible (Figure 35). The behavior of both intercalators was expected from bibliography since ethidium bromide can be easily released from its complexed form with nucleic acid after the addition of salts (Waring et al, 1965) and GelRed has such a structure making it a more stable intercalator. Finally, direct visualization of the elongated DNA molecules by AFM constitutes an easy and reproducible complementary method for an extra verification of the elongation.

In conclusion, the quartz crystal microbalance (QCM) is a non-invasive, nanogram sensitive technique, which can be used to study structural changes of DNA biomolecules at the interface. Apart from the ability to discriminate between different conformational structures, even during hybridization, here we prove that the QCM-D can also sense the elongation of DNA molecules induced by intercalators. In constant to the previously used techniques for DNA-drug interactions, which show their own advantages, this can lead to the development of highly sensitive acoustic detection platforms for DNA-drug analysis, in which the structural changes of DNA induced by the binding of small molecules are crucial. This may well be an important finding for acoustic biophysics and Nano biotechnology. Toward this direction it is anticipated that further study and understanding of the effect of other types of external agents on DNA may be proven necessary.

ACKNOWLEDGMENTS

The author thank the Physics department of the University of Crete for the kind loan of the AFM NanoScopeIIIa microscope system. Ms. Katerina Tsagaraki from Physics department and Dr Pablo Mateos-Gil from Biosensors lab, University of Crete, are also gratefully acknowledged for carrying out the AFM experiments. Credits to Professor Vontas and his laboratory from the Biology department, University of Crete and more specific to Dimitra Tsakireli are given for the support and loan of the UV-Vis SpectraMax M2 spectrophotometer. Also many thanks are given to Maria Megariti and Dr Giwrgos Papadakis for their help with the PCR reactions. Finally, I would like to thank Professor Ms. Electra Gizeli, who gave me the opportunity to work on a very interesting topic and in a very collaborating laboratory and the researcher Dr Tsortos Achilleas who was always willing to help me throughout my master thesis.

REFERENCEES

Aleksic M and Kapetanovic V. An Overview of the Optical and Electrochemical Methods for Detection of DNA – Drug Interactions. Acta Chim. Slov (2014), 61, 555–573

Benevides J and Thomas G. J. Local Conformational Changes Induced in B-DNA by Ethidium Intercalation. Biochemistry (2005), 44, 2993-2999

Berge T, Jenkins NS, Hopkirk RB, Waring MJ, Edwardson JM, Henderson RM. Structural perturbations in dna caused by bisintercalation of ditercalinium visualised by atomic force microscopy. Nucl Acids Res (2002) 30 (13):2980–2986

Breslauer K, Remeta D, Chou W, Ferrante R, Curry J, Zaunczkowski D, Snyder J, Marky L. Enthalpy-entropy compensations in drug-DNA binding studies (thermodynamic driving forces/drug-induced changes/probes of DNA conformation) Proc. Nati. Acad. Sci. USA Vol. 84, pp. 8922-8926, Biochemistry 1987

Chib R, Raut S, Sabnis S, Singhal P, Gryczynski Z, Gryczynski I. Associated Anisotropy Decays of Ethidium Bromide Interacting with DNA. Methods Appl Fluoresc. 2014; 2(1): 015003

Crisafuli F. A. P., Ramos E. B., Rocha M. S. Characterizing the interaction between DNA and GelRed fluorescent stain. Eur Biophys J (2015) 44:1–7

Dixon M. Quartz Crystal Microbalance with Dissipation Monitoring: Enabling Real-Time Characterization of Biological Materials and Their Interactions. Journal of Biomolecular Techniques 19:151–158 (2008)

Dougherty G and Pigram W. J. Spectroscopic Analysis of Drug-Nucleic Acid Interaction. Critical Reviews in Biochemistry, (1982) 12:2, 103-132,

Douthart R. J, Burnett J. P, Beasley F. W and Frank B. H. Binding of Ethidium Bromide to Double-Stranded Ribonucleic Acid. Biochemistry, VOL. 12, NO. 2, (1973)

Egli M., Williams L.D., Frederick C.A., Rich A. DNA-nogalamycin interactions. Biochemistry, 30 (1991), pp. 1364–1372

Ehrlich P. Ueber Salvarsan. Münchener medizinische Wochenschrift 58: 2481-2486. (1911)

Fei M; Leung W. Methods of Using Dyes in Association with Nucleic Acid Staining or Detection and Associated Technology (2006) Patent US20060211029

Furusawa H, Nakayama H, Funasaki M, Okahata Y. Kinetic characterization of small DNA-binding molecules interacting with a DNA strand on a quartz crystal microbalance. Analytical Biochemistry 492 (2016) 34-42

Gaugain B, Barbel J, Capelle N, Roques B and Le Pecq J. Binding Interaction of an Ethidium Homodimer and an Acridine Ethidium Heterodimer. Biochemistry. VOL. 17, NO. 24, (1978)

Glazer N, Peck K, and Mathies R A. A stable double-stranded DNA-ethidium homodimer complex: application to picogram fluorescence detection of DNA in agarose gels. Proc. Natl. Acad. Sci. USA Vol.87, pp. 3851-3855, (1990)

Günther K, Mertig M, Seidel R. Mechanical and structural properties of yoyo-1 complexed DNA. Nucl Acids Res 38(19):6526–6532(2010)

Höök F, Kasemo B, Nylander T, Fant C, Sott K, Elwing H. Variations in coupled water, viscoelastic properties, and film thickness of a Mefp-1 protein film during adsorption and cross-linking: a quartz crystal microbalance with dissipation monitoring, ellipsometry, and surface plasmon resonance study. Anal Chem. 2001; 73(24):5796-804.

Höök F, Rodahl M, Keller C, Glasmäster K, Fredriksson C, Dahlqvist P, Kasemo B. The Dissipative QCM-D Technique: Interfacial Phenomena and Sensor Applications for Proteins, Biomembranes, Living Cells and Polymers EFTF - IEEE IFCS, Volume 2, 13-16 (1999) Page(s):966 - 972

Jain SC and Sobell HM. Visualization of drug-nucleic acid interactions at atomic resolution. VIII. Structures of two ethidium/dinucleoside monophosphate crystalline complexes containing ethidium: cytidylyl (3'-5') guanosine. J Biomol Struct Dyn. 1984 (5):1179-94.

Johnson NP, Butour JL, VillaniG, Wimmer FL, Defais M and Pierson V. Metal antitumor compounds: the mechanism of action of platinum complexes. Prog Clin Biochem Med (1989) 10, 1-24

Kelly J M, Tossi A B, McConnell D J and OhUigin C. A study of the interactions of some polypyridylruthenium (II) complexes with DNA using fluorescence spectroscopy, topoisomerisation and thermal denaturation. Nucleic Acids Res. 1985 Sep 11; 13(17): 6017–6034

Lauria A, Montalbano A, Barraja P, Dattolo G, Almerico AM. DNA minor groove binders: an overview on molecular modeling and QSAR approaches. Curr Med Chem. 2007; 14 (20):2136-60.

LePecq J.B and Paoletti C. A Fluorescent Complex between Ethidium Bromide and Nucleic Acids Physical-Chemical Characterization J. Mol. Biol. (1967) 27, 87-106

Lerman LS. Structural considerations in the interaction of DNA and acridines. J Mol Biol. 1961 (3): 18-30.

Leroy L and James W. On the degree of unwinding of the dna helix by ethidium ii. Studies by electron microscopy. Biochimica et Biophysica Acta, 395 (1975) 405—412

Lipinski C.A. Lead- and drug-like compounds: the rule-of-five revolution. Drug Discovery Today Technol. (2004) 1: 337-341.

Liu C, Chen F. Actinomycin D binds strongly, dissociates slowly at the dGpdC site with flanking T/T mismatches. Biochemistry, 35 (1996), pp. 16346–16353

Macgregor B. R, Clegg R and Jovin T. Viscosity Dependence of Ethidium-DNA Intercalation Kinetics Biochemistry VOL. 26, NO. 13, (1987)

Mateos-Gil P, Tsortos A, Velez M and Gizeli E. Monitoring structural changes in intrinsically disordered proteins using QCM-D: application to the bacterial cell division protein ZipA. Chem. Commun., 2016, 52, 6541—6544

Muller W, Crothers M. D. Interactions of Heteroaromatic Compounds with Nucleic Acids 1. The Influence of Heteroatoms and Polarizability on the Base Specificity of Intercalating Ligands Eur. J. Biochem. 54,267-277 (1975)

Newton BA. The mode of action of phenanthridines: the effect of ethidium bromide on cell division and nucleic acid synthesis. J Gen Microbiol. 1957 (3):718-30.

Nordmeier E. Absorption Spectroscopy and Dynamic and Static Light-Scattering Studies of Ethidium Bromide Binding to Calf Thymus DNA: Implications for Outside Binding and Intercalation J. Phys. Chem. (1992), 96, 6045-6055 6045

Okahata Y, Matsuzaki Y and Ijiro K. Detection of intercalation behaviors of dyes in DNAs using a quartz-crystal microbalance Sensors and Actuators B, 13-14 (1993) 380-383

Papadakis G, Skandalis N, Dimopoulou A, Glynos P, Gizeli E. Bacteria Murmur: Application of an Acoustic Biosensor for Plant Pathogen Detection. PLoS ONE 10(7): e0132773 (2015)

Papadakis G, Tsortos A, Bender F, Ferapontova E and Gizeli E. Direct Detection of DNA Conformation in Hybridization Processes. Anal. Chem. 2012, 84, 1854−1861

Peacocke A.R and Skerrett J.N.H. The interaction of aminoacridines with nucleic acids. Transactions of Faraday Society Vol 52: 261-279 (1955)

Pope L, Allen S, Davies M, Roberts C, Tendler S and Williams P. Probing DNA Duplex Formation and DNA-Drug Interactions by the Quartz Crystal Microbalance Technique. Langmuir (2001), 17, 8300-8304

Rawle R, Selassie C and Johal M. Creation of Mammalian Single- and Double-Stranded DNA Surfaces: A Real-Time QCM-D Study. Langmuir, 2007, 23 (19), pp 9563–9566

Rescifina A., Zagni C., Varrica M., Pistarà V. and Corsaro A. Recent advances in small organic molecules as DNA intercalating agents: Synthesis, activity, and modeling. European Journal of Medicinal Chemistry 74 (2014) 95-115

Rocha M. S, Ferreira M. C. and Mesquita O. N. Transition on the entropic elasticity of DNA induced by intercalating molecules THE JOURNAL OF CHEMICAL PHYSICS 127, 105-108 (2007)

Sassolas, A.; Leca-Bouvier, B. D.; Blum, L. DNA biosensors and microarrays. J. Chem. Rev. 2008, 108 (1), 109−139

Sauerbrey, G. Z. The use of quartz oscillators for weighing thin layers and for microweighing. (1959) Phys, 155, 206–222.

Scatchard G. The attractions of proteins for small molecules and ions. Annals New York Academy of Science. 51:660-672 (1949)

Su X, Ying-Ju W, Wolfgang K. Comparison of surface plasmon resonance spectroscopy and quartz crystal microbalance techniques for studying DNA assembly and hybridization Biosensors and Bioelectronics 21 (2005) 719–726

Tanious F. A., Yen S. F. and Wilson W. D. Kinetic and equilibrium analysis of a threading intercalation mode: DNA sequence and ion effects. Biochemistry, 1991, 30 (7), pp 1813–1819

Tsortos A, Papadakis G, and Gizeli E. On the hydrodynamic nature of DNA acoustic sensing. Anal. Chem. 2016, 88, 6472−6478

Tsortos A, Papadakis G, Gizeli E. Shear acoustic wave biosensor for detecting DNA intrinsic viscosity and conformation: A study with QCM-D. Biosensors and Bioelectronics 24 (2008) 836–841

Vardevanyan P.O, Antonyan A.P. Parsadanyan M.A., Davtyan H.G. and Karapetyan A.T. The binding of ethidium bromide with DNA: interaction with single- and double-stranded structures EXPERIMENTAL and MOLECULAR MEDICINE, Vol. 35, No. 6, 527-533, December 2003

Voinova M. V., M. Rodahl, M. Jonson and B. Kasemo Viscoelastic Acoustic Response of Layered Polymer Films at Fluid-Solid Interfaces: Continuum Mechanics Approach. Physica Scripta (1999)

Wainwright M. Acridine—a neglected antibacterial chromophore. J Antimicrob Chemother (2001) 47 (1): 1-13

Waring M. J. Drugs which affect the Structure and Function of DNA. Nature 219, 1320 - 1325 (1968)

Waring M.J. Complex formation between ethidium bromide and nucleic acids. J Mol Biol. 1965 (1):269-82.

Watson J.D, Crick F.H.C. Molecular Structure of Nucleic Acids: A Structure for Deoxyribose Nucleic Acid. Nature 171, 737-738 (1953)

Wolny P, Spatz J and Richter R. On the Adsorption Behavior of Biotin-Binding Proteins on Gold and Silica. Langmuir 2010, 26(2), 1029–1034

Wu F, Fei-Yan X, Yu-Mei W & Jong-In H. Interaction of a New Fluorescent Probe with DNA and its Use in Determination of DNA J Fluoresc (2008) 18:175–181

Xiao J, Lin J and Tian B. Denaturation temperature of DNA Phys. Rev. E 50, 5039 (1994)

Yang A, Rawle R, Selassie C and Johal M. A Quartz Crystal Microbalance Study of Polycation-Supported Single and Double Stranded DNA Surfaces. Biomacromolecules 2008, 9, 3416–3421

Zhang X., Chu S.S., Ho J.R., Grigoropoulos C.P. Excimer laser ablation of thin gold films on a quartz crystal microbalance at various argon background pressures Appl. Phys. A 64, 545–552 (1997)

.